THESIS FOR THE DEGREE OF DOCTOR OF PHILOSOPHY

Laser-welded corrugated core steel sandwich bridge decks

PETER NILSSON STRAND

Department of Architecture and Civil Engineering
Division of Structural Engineering
Lightweight Structures
CHALMERS UNIVERSITY OF TECHNOLOGY
Gothenburg, Sweden 2020

Laser-welded corrugated core steel sandwich bridge decks

PETER NILSSON STRAND

ISBN 978-91-7905-261-4
Doktorsavhandlingar vid Chalmers tekniska högskola
Ny serie, nr 4728
ISSN 0346-718X

Thesis for the degree of Licentiate of Engineering
Department of Architecture and Civil Engineering
Division of Structural Engineering
Lightweight Structures
Chalmers University of Technology
SE-412 96 Gothenburg
Sweden
Telephone: + 46 (0)31-772 1000
www.chalmers.se

Cover: Laser-welded corrugated core steel sandwich panel; real structure (left) and numerical result (right).

Chalmers Reproservice
Gothenburg, Sweden, 2020

To Lovisa, Matilda and Olle.

Laser-welded corrugated core steel sandwich bridge decks

PETER NILSSON STRAND
Department of Architecture and Civil Engineering
Division of Structural Engineering, Lightweight Structures
Chalmers University of Technology

ABSTRACT

Steel bridge decks are often used for applications when a lightweight structure is sought for. Conventional orthotropic steel decks suffers from drawbacks in several aspects, including high production costs and durability problems. Corrugated Core Steel Sandwich Panels (CCSSPs) have shown a good potential to become the next generation lightweight bridge decks with enhanced structural properties compared to its predecessor. The work presented in this thesis aims at verifying CCSSPs for bridge applications and to gain an increased understanding of their structural behaviour. Even though considerable research effort related to all-steel sandwich panels has been made, focus in previous work has been on web-core sandwich panels. Very little work has been devoted to corrugated core panels, particularly with reference to bridge deck applications.

In this work, a production process is presented for the novel CCSSP. Four demonstrator panels, of C-Mn and Duplex stainless steel are produced. The production-dependent geometric properties of the panel are measured, and it is concluded that the production process give good quality of the panel. Within the measured variation of the geometric properties, the impact of this variation on the fatigue-relevant stresses is studied using numerical analyses. As an example, the results show strong impact of the weld-width and possible misalignment of the welds.

Fatigue is a highly important factor for steel bridge decks and it has a strong relation to durability and strength requirements that are put on the deck. Here, the fatigue-strength of laser-welds in CCSSPs is assessed using experiments and numerical analyses. The results show alignment to other previously performed fatigue tests, and that with respect to the effective notch stress approach, the current recommendations given in design codes can be used, with a presented restriction. In addition to the small-scale cell specimens, a panel-specimen is also tested under fatigue loading. The results from this test demonstrate high fatigue-performance of the CCSSP.

To ensure that structural requirements concerning stiffness and strength are satisfied, reliable analysis methods are needed. To find an optimal bridge deck topology, and to run many load-cases, these analyses also needs to be time-efficient. In this thesis, two approaches with these targets are evaluated using numerical analyses. The results show that it is possible to accurately predict stresses using a deformation driven sub-modelling approach. Incorporation of the deformability of the weld region is shown to have a high impact on the state of stress in the welds, and a modelling technique is presented in this aspect. In addition, equivalent stiffness properties of CCSSPs are investigated and derived herein. A general conclusion from this work is that the results validate the feasibility of using CCSSPs for bridge deck applications.

Keywords: Bridge deck, steel sandwich, laser-weld, corrugated core, fatigue.

PREFACE

The work presented in this thesis was performed at Chalmers University of Technology, Department of Structural Engineering, Lightweight Structures, between January 2015 and December 2019. It was performed as a collaboration between Chalmers and the company WSP. This thesis is a further development of the work presented in the Licentiate thesis: *Laser-welded corrugated core steel sandwich panels for bridge application*. This work was funded by: Swedish Transportation Administration, Swedish research agency Vinnova and the Norwegian Public Roads Administration as a part of the project "Costal highway route E39". Your support is greatly appreciated.

First, I would like to thank my supervisor, Associate Professor Mohammad Al-Emrani, for his continuous support and shearing of knowledge during this period. My co-supervisor, Rasoul Atashipour, PhD, your work is highly valued. My former and current managers at WSP; Roland Olsson and Daniel Ekström, thank you so much for this opportunity and your support.

During the phase of production of the demonstrator panels, several parts contributed with knowledge and enthusiasm; Joakim Hedegård at Swerim AB, Outukompu Stainless Steel and Tore Roppen and Simon Sundal at Kleven Verft AS, your efforts were crucial and are appreciated. Furthermore, all the partners in the research project INNODEFAB; your contributions are highly valued. Sebastian Almfeldt and Anders Karlsson, your support on the experimental work is very much appreciated.

Finally, I would like to direct all my love to Lovisa, Matilda and Olle, for all your patience and support.

Gothenburg, 2020

Peter Nilsson Strand

LIST OF PUBLICATIONS

This thesis is based on the work contained in the following papers:

PAPER I

P. Nilsson, J. Hedegård, M. Al-Emrani and S.R. Atashipour. *The impact of production-dependent geometric properties on fatigue-relevant stresses in laser-welded corrugated core steel sandwich panels,* Welding in the world. Vol 63, pp 1801-1818, August 2019.

PAPER II

P. Nilsson, M. Al-Emrani and S.R. Atashipour. *Fatigue-strength assessment of laser-welds in corrugated core steel sandwich panels,* Journal of Constructional Steel Research, Vol 164, October 2019.

PAPER III

P. Nilsson, S.R. Atashipour and M. Al-Emrani. *Corrugated core sandwich panels: numerical modelling strategy for structural analysis*. Submitted for publication.

PAPER IV

P. Nilsson, M. Al-Emrani and S.R. Atashipour, *Transverse shear stiffness of corrugated core steel sandwich panels with dual weld lines*, Thin-Walled Structures, Vol 117, pp 98-112, August 2017.

PAPER V

P. Nilsson, M. Al-Emrani and S.R. Atashipour, *A numerical approach to the rotational stiffness of stake welds.* Proceedings of EUROSTEEL 2017, pp 489–498, Copenhagen, Denmark

AUTHOR'S CONTRIBUTIONS TO JOINTLY PUBLISHED PAPERS

The contribution of the author of this thesis to the appended papers is described here.

I. Responsible for the preparation of the manuscript for the paper, apart from Section 2. The author performed the literature review, defined the setup for parametric study, executed the parametric study and was responsible for the conclusions. Furthermore, the author was responsible for all preparations of specimens before measurements and executed all measurements except for the weld widths and plate gaps of Beam 1. Also, the author led the work of the production of the panels, together with experts from the field of manufacturing and welding technology.

II. Responsible for the preparation of the manuscript for the paper. The author performed the literature review, defined the test setups together with co-authors, executed the tests, and performed the measurements and numerical analyses.

III. The author performed the literature review, defined the setup for the numerical simulations and was responsible for the conclusions. The author prepared the manuscript for the paper together with the second author.

IV. Responsible for the preparation of the manuscript for the paper. The author performed the literature review, defined the setup for the analytical solution, executed the derivation and verification and was responsible for the conclusions.

V. Responsible for the preparation of the manuscript for the paper. The author performed the literature review, defined the setup for the numerical solution, executed the parametric study, executed the regression analyses and was responsible for the conclusions.

CONTENTS

1 INTRODUCTION

1.1 BACKGROUND

Bridges are structures affecting the social, economic and environmental aspects of sustainability. Within the research project Pantura [1], European bridge owners responded to a questionnaire regarding bridge demographics, maintenance and costs, etc. Statistical analysis of the responses showed that about 45% of all rehabilitation activities on bridges are devoted to repair and replacement of steel decks and concrete decks in composite bridges; see Pantura D5.3 [2]. Thus, bridge decks are vulnerable and highly relevant with respect to the life-cycle perspective of a bridge. For this reason; structural solutions for bridges that are sustainable are sought for by governmental transport administrations world-wide.

The deck of a bridge has multiple functions in terms of load bearing. Figure 1 illustrates three types of load-bearing functions of a bridge deck. It shall withstand the locally applied load from a wheel pressure (see Figure 1a, for the specific case of a conventional steel bridge deck). Moreover, it shall effectively distribute the load to the supporting structure, i.e girder system or abutment (see Figure 1b). Furthermore, it can also be utilised in composite action as a flange in the main load-carrying structure (see Figure 1c). Thus, versatile structural demands are placed on bridge decks; to carry load locally, to distribute them effectively through plate action and to withstand high membrane forces from global action. The choice of bridge deck type for a new structure or deck replacement in an existing bridge, is based on different owner priorities. During the above mentioned research project Pantura [1], four European bridge owners listed their order of priority and the results showed that costs and construction time were rated high.

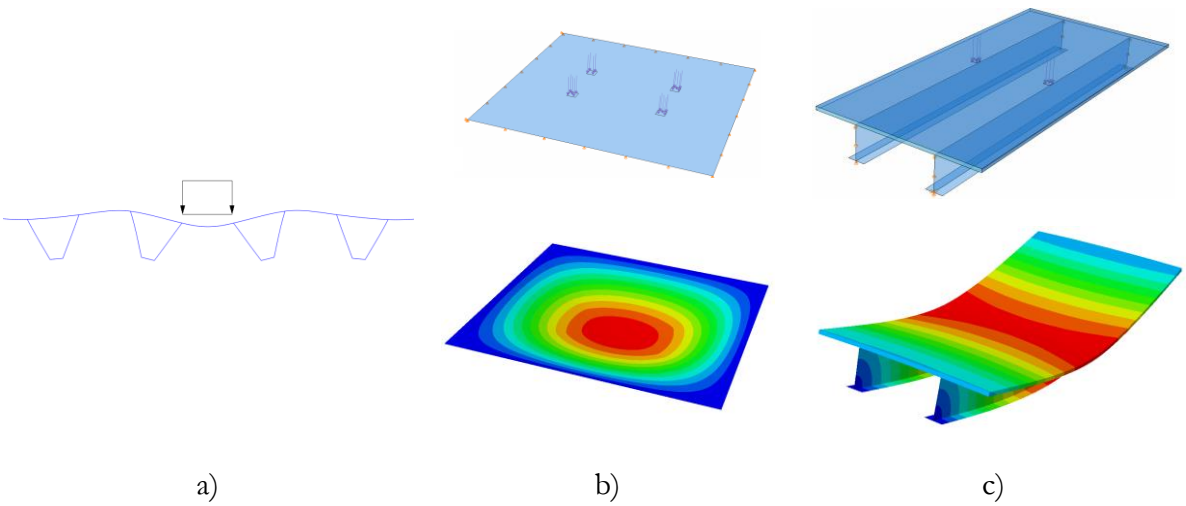

a) b) c)

Figure 1. Bridge deck actions; a) local action due to wheel pressure, b) plate action for load distribution, c) flange action for global stiffness.

Due to the fact that bridge decks are important parts for the whole bridge structural behaviour and important for the total bridge economy, they have been constant subjects of research and innovation. Today concrete bridge decks are by far the most common type of

solution in Sweden. Their main benefits are that the knowledge of their design, production and long-term performance is well documented and known within the industry. However, they are mass-intensive and have a large CO_2-footprint. Aluminium decks have been used to a relatively wide extent in bridge rehabilitation. Among others, Arrien et al. [3] reported that aluminium bridge decks are lightweight, weighing only one tenth of a concrete bridge deck and that they are competitive by an ease of on-site assembly. Nevertheless, there exists drawbacks as low stiffness, non-composite action with the underlying main structure, extensive pavement maintenance in the joint region and a high initial cost. For these reasons, aluminium bridge decks are not used in Sweden as often today as for twenty years ago. Fiber reinforced polymer bridge decks have been developed and used for the last decade, see Mara et al. [4]. They are very lightweight and have a high fatigue and corrosion resistance. Nevertheless, the initial costs are high and their long-time performance has not yet been fully investigated. Sandwich Plate System (SPS) bridge decks, developed by Intelligent Engineering [5], benefit from a high stiffness and low weight, and have been used in several countries such as US, China, Germany and Canada [5]. The deck basically consists of two steel face sheets interconnected with an elastomer core. Harris [6] stated that the lack of design-models is the main obstacle for a wider implementation of SPS bridge decks. However, there is a lack of information in the literature regarding cost-efficiency and long-term performance of the concept as well.

Conventional Orthotropic Steel Decks (OSDs) (see Figure 2) possess a high stiffness-to-weight ratio in their longitudinal direction and are thereby an attractive solution for many bridge applications. In their original geometric shape they consisted of flat stiffeners, and then evolved to stiffeners with a bottom flange and in the conventional shape of today the stiffeners have a trapezoidal shape. However, OSDs are labor-intensive to produce (see Kolstein [7]) and suffer from premature deterioration that leads to high investment and maintenance costs, respectively. The premature deterioration originates from a low local stiffness in the direction orthogonal to the stiffeners that causes large deformations and thereby occurrence of cracks in the pavement (Kolstein [7]). Furthermore, OSDs are fatigue sensitive (see Kolstein [7], Leendertz and Kolstein [8], Wolchuk [9], Qian and Abruzzese [10]). Due to the high investment and maintenance costs an OSD is in general only considered as an economically feasible option for cases where the structural weight is of the outermost importance; see e.g. Bright and Smith [11] or Kolstein [7]. Bright and Smith [11] stated that an OSD is about four times as expensive as a concrete deck and that the fabrication costs of the steel deck often exceed the material costs.

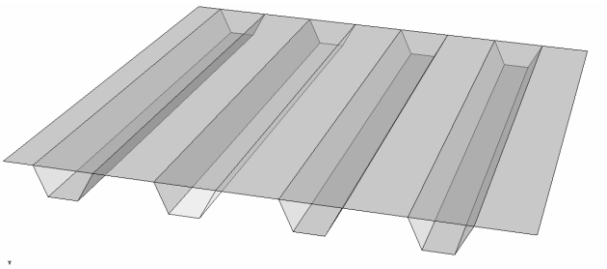

Figure 2. Conventional OSD with longitudinal trapezoidal stiffeners.

The core of an all-steel sandwich panel may be produced with different shapes. A range of possibilities of core types are shown in Figure 3. All cross-section shapes in Figure 3, except for E, can be produced by laser-welding (E in Figure 3 shows an extruded aluminium section). All the cross sections in Figure 3 are orthotropic and have approximately equal bending stiffness in the longitudinal and transversal direction. What separate the core geometries are their material consumption, shear stiffness in the direction orthogonal to the core (i.e. the weak direction) and production aspects. The inclination of the core leg for the Corrugated Core Steel Sandwich Panel (CCSSP, A in Figure 3), gives it an increased shear stiffness in the weak direction compared to those with straight cores, for instance B (web-core) and G (C-core) of Figure 3 (see e.g. Lok and Cheng [12]). Thus, the inclination of the core leg yields an enhanced two-way load-carrying behaviour, i.e. plate action, beneficial for several bridge applications. Furthermore, enhanced plate action increases the spread of a concentrated load (e.g. wheel pressure). However, in general, the CCSSP consumes more material than the web-core and C-core sandwich panel. Thus, the most material effective type of core configuration depends on the type of loads and Boundary Conditions (BCs). For a bridge deck supported by longitudinal and transversal girders, the pronounced plate action of the corrugated core is beneficial.

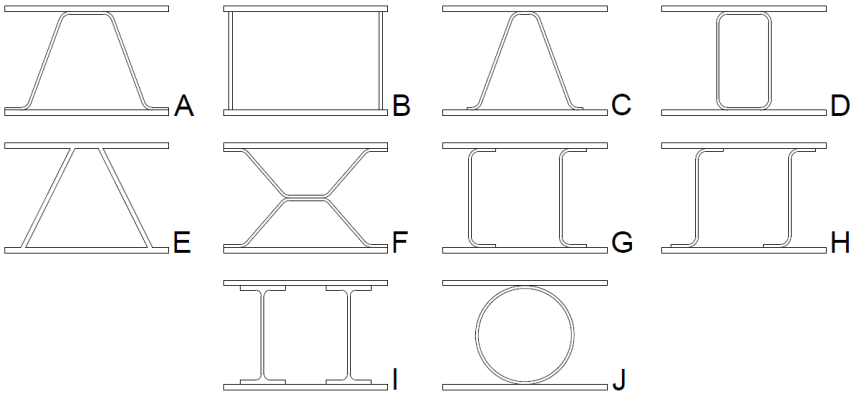

Figure 3. 10 possible structural core sandwich panel geometries [13].

For applications where, conventional orthotropic bridge decks are used today, an all-steel sandwich panel bridge deck can be used with benefits related to material consumption and manufacturing. Movable bridges (see Figure 4) and a deck-plate in a box-girder of a cable-supported bridge, are two examples of that. Furthermore, Dackman and Ek [14] showed that for medium-span bridges - which in Sweden are commonly made of steel girders with concrete decks in composite action - a CCSSP bridge deck could substitute the concrete deck, resulting in a bridge that can be launched in one piece. This yields a promising bridge concept, especially in urban areas, where minimised erection time results in reduced costs related to traffic disturbance. Ungermann and Russe [15] proposed usage of a sandwich panel bridge (without girders) for road traffic, simply supported on two edges. This is a concept where complete prefabrication of the bridge superstructure is possible and where the light weight of the bridge yields an ease of on-site construction. For this concept, transportation and the challenge to perform on-site joining of panels, sets the limitation on the bridge size. In this segment of the bridge stock, pre-stressed timber bridges, concrete slab bridges and steel and soil composite bridges are the main competitors. From a life-cycle perspective, a stainless

steel sandwich panel concept can be cost- and CO2-effective for these bridges. All-steel sandwich panels have today not yet been widely applied in bridges. The only known bridge applications (to the best of the authors knowledge) are a few minor local bridge-projects in connection to the development of I-core sandwich panels at the German ship-yard Mayer Werft in Papenburg (see Roland and Metschkow [17], Roland and Reinert [23] and Roland et al. [16]–[18]).

Figure 4. Possible bridge deck application for all-steel sandwich panel; a bascule bridge [19].

All metal sandwich panels can be manufactured using different joining techniques such as mechanical fastening, resistance spot welding, adhesive bonding, extrusion or laser-based welding. The earliest proposals of all-steel sandwich panels used mechanical fastenings in the form of rivets, as Libove and Hubka [20] with focus on applications for the aeronautical industry. During the late 1980s a research study was performed at the university of Manchester on resistance spot-welded corrugated steel sandwich panels, see Tan et al. [21]. Static- and fatigue loads were investigated by numerical analysis and experiments for adhesively bonded corrugated core steel sandwich beams by Knox et al. [22] and extruded aluminium sandwich plates has been addressed by e.g. Lok and Cheng [23]. Laser-welding makes it possible to create a continuous and robust connection between the core and the face plates. In the 1980s the development of laser-welded steel sandwich panels was led by the US navy (see Reutzel et al. [24] and Sikora and Dinsenbacher [25]). Since then, the development has been led by European research with application in ship-building in, for instance, Finland (Romanoff and Kujala [26], Romanoff [27], Jelovica [28] and Frank et al. [26]–[29]), Poland (Kozak [30]) and Germany (Roland et al. [18]). Several European projects addressing the topic of laser-welded steel sandwich panels has been performed; see e.g. SANDWICH [31] and SANDCORE [32]. Application of steel sandwich panels can be found in a variety of industries as sub-way trains [33], fortification systems [34], ro-ro deck ramp in a ship [30], gravel truck container [35] etc.

Laser-welded all-steel sandwich panels have been proposed for bridge deck applications by several researchers (see Bright and Smith [11], Caccese and Yourulmas [36], Klostermann [37] and Nilsson and Al-Emrani [13]). A laser-welded CCSSP is shown in Figure 5a. All-steel sandwich panels can be produced by two main laser-based welding processes. Either a pure laser process is adopted, or a hybrid-process involving conventional arc-welding. Figure 5b

shows a robotic laser-welding equipment. The main property of the laser-based welding processes that enable the single-sided welding is the high energy density of the laser beam, making a deep penetration possible. In addition to the atomised production of the deck itself, connections to the supporting structure (transverse girders) is more straight-forward when CCSSPs are used compared to OSDs. Conventional OSDs are joined to the web of transverse girders with a complex procedure involving a curved welding path that today most often is performed manually. Also, in order to manufacture this connection, the OSD solution demands cut-outs to be made in the transverse girder. The corresponding connection for a CCSSP can be a straight weld, see Figure 5c for a comparative illustration. All-steel sandwich panels are weight-efficient compared to conventional stiffened plate solutions and material savings ranging from 10-50% are reported in the literature for both bridge and ship structures (see e.g. Beneus and Koc [19], Kujala and Klanac [38], Roland and Reinert [17] and Kujala et al. [39]). These weight savings are not on the deck alone, but the weight decrease of the surrounding structure working in full composite action is also included. The structural efficiency of CCSSPs in comparison with conventional orthotropic decks stems from three key aspects: an increased bending stiffness in the longitudinal directions of the core due to a shift of the neutral axis, an increase of the bending stiffness in the perpendicular direction due to a sandwich effect also in that direction and an increased efficiency when the deck is utilised as a flange due to a less pronounced shear-lag effect, see Figure 5d-f.

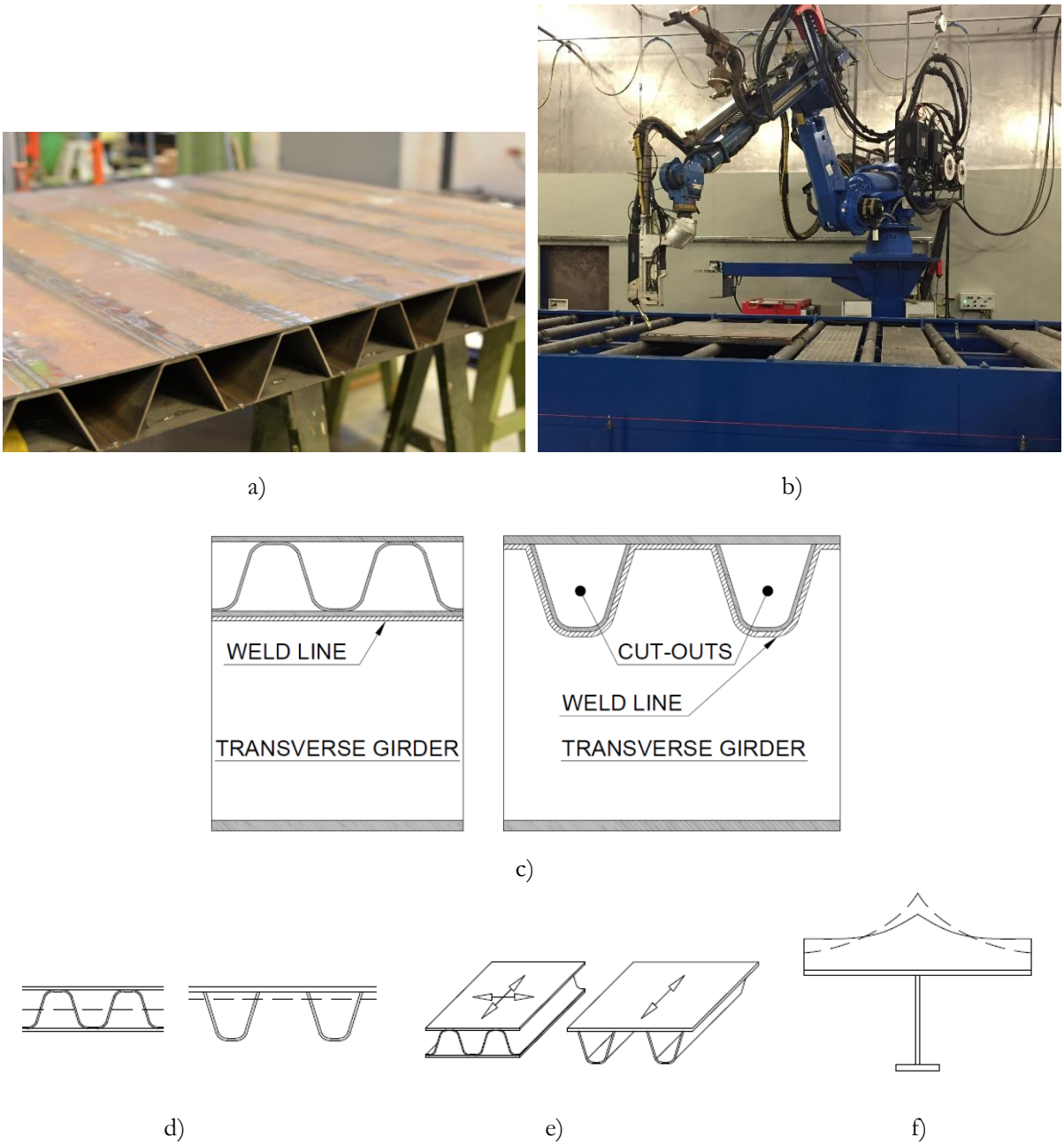

Figure 5. a) Laser-welded corrugated core steel sandwich panel, Nilsson et al. [40], b) laser-welding equipment, photo: Kleven Verft AS, c) comparison of deck to transvers girder connection between all-steel sandwich panel (left) and conventional stiffened plate (right) [13] d) increased bending-stiffness in the main direction, e) increased 2-way load distribution f) shear-lag comparison (dashed = conventional, solid = sandwich panel).

Regarding manufacturing of laser-welded all-steel sandwich panels, several authors have reported, either regarding the production of panels or on work that includes produced panels e.g. for I-core ([16], [41]–[43]) and V-core ([44], [45]), see Figure 4c. However, manufacturing of laser-welded CCSSPs, with a core-to-face joint geometric configuration with dual weld-lines, continuous core, and plate thicknesses that are relevant for bridge applications, has to the knowledge of the author not been addressed previously. In addition has this panel type not been produced using Duplex stainless steel plates.

In steel bridges in general, and more specifically in steel bridge decks, fatigue performance is of high importance to ensure a safe structure during its service life. In a bridge girder, the fatigue-sensitive welded details are subjected to stress cycles originating mainly from the global deformations, i.e. bending or shearing of the girder. In addition to this global action, a bridge deck is subjected to stress cycles from the direct contact with heavy wheel pressures. The local wheel pressure has in general shorter influence lengths, causing a large number of load-cycles per vehicle passage and it is thereby an important influencing factor in the fatigue design calculations, making the deck the most fatigue-exposed part of a bridge. The fatigue-strength of laser-welds has been investigated by several authors with a focus on joints in web-core sandwich panels (e.g. Frank [29], Fricke et al. [42], Ungermann and Russe [15]). However, to the knowledge of the author, there exists no work related to the fatigue strength of CCSSPs in the literature. Producing a welded structure yields a natural geometric variation of the joints that are produced. In addition to the fatigue strength, the impact of production dependent geometric properties on the fatigue performance has not been addressed previously for CCSSPs.

One aspect that has been the target for research previously is structural analysis of laser-welded sandwich panels. This concerns a methodology that enables stress predictions in all the constituent members of the panel, i.e. the face plates, core and welds. This work has mainly been attributed to web-core sandwich panels by e.g. Klostermann [37], Romanoff [27] or Karttunen [46], [47]. However, this aspect has previously not been investigated for CCSSPs for bridge application. In relation to this, there has been very limited work related to structural analysis methodologies that are verified to be used in design or optimisation situations where the panel is connected to a supporting structure, i.e. where the panel is serving as both a deck that distributes forces locally and to the supporting structure, and a flange that is subjected to membrane action, see Figure 1. The structural analysis of a panel often includes the average stiffness properties of the considered panel. For CCSSPs, the elastic stiffness properties was derived by Libove and Hubka [20]. However, this work relates to panels using a single weld line per core-to-face connection. The work that is presented in this thesis relates to CCSSPs that has dual weld-lines per core-to-face connection. For this configuration, there exists a need to investigate the equivalent stiffness components.

1.2 AIM AND OBJECTIVE

CCSSPs has, as it was mentioned in sub-section 1.1, shown great potential to be weight-efficient next generation steel bridge decks. However, this bridge concept is new and existing knowledge in the field is limited in several aspects. The overall aim of this thesis is *to study and verify the feasibility of CCSSPs for bridge deck application and provide a basis for evaluating their structural behaviour*. Figure 6 provides an overview of the different parts that are included in the scientific work. The specific objectives of each part are presented and motivated below.

PRODUCTION

To the knowledge of the author, CCSSPs have not been previously produced in a large scale. In this respect, three main objective were identified early in the research work. These are:

- to demonstrate the manufacturability of CCSSPs with dual weld-lines (Paper I),
- to study the natural variation of the production-dependent geometric properties of the core-to-face joint (Paper I), and
- to determine the impact of this variation on fatigue-relevant stresses in the constituents of CCSSPs (Paper I).

FATIGUE

Considering steel bridges, fatigue is a highly important topic in order to ensure a safe and durable structure. On the topic of fatigue, the following objectives are identified:

- to investigate the fatigue strength of laser-welds in CCSSPs for conventional C-Mn structural steel and Duplex stainless steel (Paper II),
- to study different fatigue failure modes in a laser-weld of a CCSSP and to identify the mechanisms leading to these failure modes (Paper II), and
- to experimentally investigate the fatigue performance of CCSSPs (Paper II).

STRUCTURAL ANALYSIS

CCSSPs with dual weld-lines, are novel and their structural behaviour has not been previously studied in detail to a wide extent. To gain an increased knowledge regarding the structural behaviour of CCSSP bridge decks, the following objectives are defined:

- to identify aspects that are significant for the design of all steel sandwich panels and in specific CCSSPs (Paper III),
- to investigate the impact of contact between the core and face plates on the state of stress in the welds (Paper I, Paper II), and
- to investigate the impact of the weld region deformations on the stiffness of CCSSPs and the state of stress in the constituent members of the cross section, including the welds (Paper III).

In order to ensure a safe and durable bridge deck, stiffness and strength design criteria needs to be fulfilled. For this verification, a reliable structural analysis approach needs to be applied. Also, for the design process of bridges, there exists a need to simplify the structural

analysis to reach manageable calculation-times, however, without considerable reduction of the level of accuracy of the results. The objectives that stem from this are:

- to evaluate different structural analysis methodologies and to assess their capabilities in predicting deformations and stresses in CCSSPs (Paper III),
- to investigate and derive analytical formulations for the equivalent stiffness properties of CCSSPs (Paper III, Paper IV), and
- to find a methodology to incorporate weld-region stiffness into structural element models (beams and shells) such that accurate estimation of the load effects in the constituent members of the cross-section (including the welds) is possible to obtain for design purposes (Paper III, Paper V).

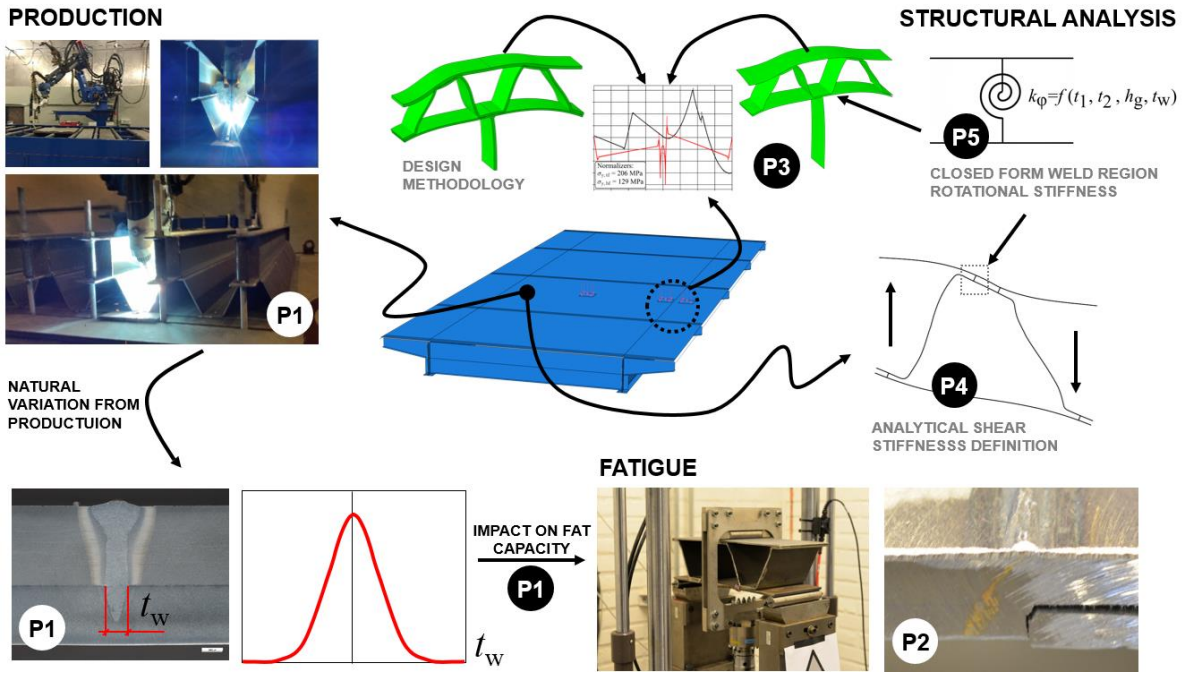

Figure 6. Superordinate topics of thesis.

1.3 METHOD

PRODUCTION

Prior to the production of the CCSSPs that was performed within this project, a literature review and parametric studies were performed. The results from these efforts, along with detailed consideration of relevant practical aspects in production, design and application, lead to the topology of the panels to be produced. In order to reach a feasible production process and thereby demonstrate the manufacturability of CCSSPs, several production tests were performed. These incorporated minor test specimens and large-scale panel-type specimens with selected topologies. The welding parameters were optimised with respect to weld quality and with the aim to reach a weld width of about 2 mm. The work related to production of the CCSSPs was performed in cooperation with experts in atomised production of steel structures (Kleven verft AS) and welding technology (Swerim AB). The nature of the structural analyses that were adopted to define the topology of the deck were approximate.

For the work concerned with the impact of variation of the production-dependent geometric parameters of the core-to-face joint in CCSSPs, measurements by optical microscope, 3-dimensional (3D) scanning and manual measurement methods were used. The parametric study in this regard was performed using numerical analysis, based on continuum elements.

FATIGUE

The work that is presented in this thesis related to the topic of fatigue in laser-welds of CCSSPs was initiated by a literature review which led to identification of knowledge gaps and the need of further studies. Fatigue was further studied experimentally via small-scale and large-scale specimens. Finite Element Analysis (FEA) was conducted on different levels in order to evaluate relevant load-effects. Before cyclic loading, static testing was performed and strains were measured on the surface of the specimens in order to validate the developed corresponding numerical model. During the cyclic load tests, the strains were measured continuously. Before and after failure of the specimens, different geometrical properties were measured by manual methods and optical microscope.

STRUCTURAL ANALYSIS

The work related to both the structural behaviour and the evaluation of structural analysis approaches for CCSSPs was initiated by a literature survey followed by numerical analyses using both continuum and structural elements. Regarding the investigations of equivalent stiffness properties, a literature review was performed. It revealed several missing elements in order to accurately predict deformations and stresses in CCSSPs, mainly regarding the weak direction transverse shear stiffness. To derive the weak direction transverse shear stiffness of CCSSPs with dual weld lines, an analytical model was developed. Verification of the analytical model was performed by numerical and experimental analyses. In order to find an appropriate model for incorporating the weld region stiffness in structural element models, comparative numerical analyses were used. The closed form solution for the magnitude of the most important weld region deformation, was derived based on a large number of numerical analyses via regression analysis.

1.4 SCOPE AND LIMITATIONS

PRODUCTION

Regarding the production of panels, both conventional C-Mn structural steel S355 and Duplex stainless steel LDX2101 are investigated. Panel-level connections and connections to a supporting structure or to other elements of a bridge (e.g. edge beams) are left outside of the scope of this work. On the subject of the impact of the production-dependent geometric properties of the core-to-face joint, only load-transfer in the weak direction of the panel is considered in the parametric study. Furthermore; three specific core-to-face joint geometric parameters, two load-cases, and three specific beam geometries are contained in the scope of this parametric study.

FATIGUE

In this thesis, the investigations that are related to fatigue, are primarily concerned with fatigue failures that occur in the region of the weld, in laser stake-welds. The fatigue experiments using "cell-specimens" are executed with loadings that produce multiaxial state of stress (normal stress and shear-stress from shear-force perpendicular to the weld-line). Thereby, the effect of shear stresses from shear-force in the direction parallel to the weld-line is not studied. As for the production, the tests are limited to steels of S355 and LDX2101. The results are assessed using the effective notch stress approach and the nominal stress approach. Other assessment methods are left outside the scope of this thesis.

STRUCTURAL ANALYSIS

The scope of this thesis, regarding the topic of structural analysis, considers the behaviour of CCSSP bridge decks in interaction with a supporting structure of longitudinal and transversal girders. Here, the deck orientation is with the decks stiff direction in parallel to the main girder. In the evaluation of the simplified modelling approaches, two approaches are investigated, denoted as the ESL approach and the sub-modelling approach. Other possible methodologies are not considered in this work. Regarding the structural analyses that are developed for the work in this thesis; filling of the panel voids, core configurations other than the corrugated core, dynamic loading and buckling are left outside of the scope of this thesis. Even though contact action of the core and face plates is investigated within this work, it is not incorporated in the work that is related to evaluation of the different structural analysis approaches.

1.5 OUTLINE

Section 1. This section gives a background to the topic of this thesis, motivates the field of research, declares the aims of the work and describes the adopted research methodologies.

Section 2. This section describes the manufacturing process for laser-welded CCSSPs and a study regarding the impact of variation of the production-dependent geometrical properties of the core-to-face joint in CCSSPs, i.e. the work of Paper I, is summarised.

Section 3. Here, the topic of fatigue strength of laser-welds in CCSSPs is addressed and the work of Paper II is summarised.

Section 4. Structural analysis is the topic of this section and the work of Papers III-V is summarised together with a literature review on this topic.

Section 5. The main conclusions from the five research papers presented within this thesis are summarised in this section.

2 MANUFACTURING

2.1 PANEL PRODUCTION

The key that enables the production of all-steel sandwich panels is a welding procedure that is capable of producing a stake weld that connect each pair of plates in the CCSSP. Paper I describes the production process of four CCSSPs. Laser-based welding processes are feasible procedures to create stake-welds. Figure 7 shows typical cross sections of two stake welds; a pure laser weld and a hybrid laser-arc weld. The hybrid process yields a wider weld due to the higher heat input and more pronounced weld reinforcement due to addition of weld material compared to the pure laser process. For the welds in Figure 7, the pure laser was executed by using 9kW laser power at 600mm/min welding speed, joining an 8 to a 6mm plate. The corresponding numbers for the hybrid process was 9kW laser power, 800mm/min and 6.7kW MIG/MAG-power for joining a 6 to a 5mm plate.

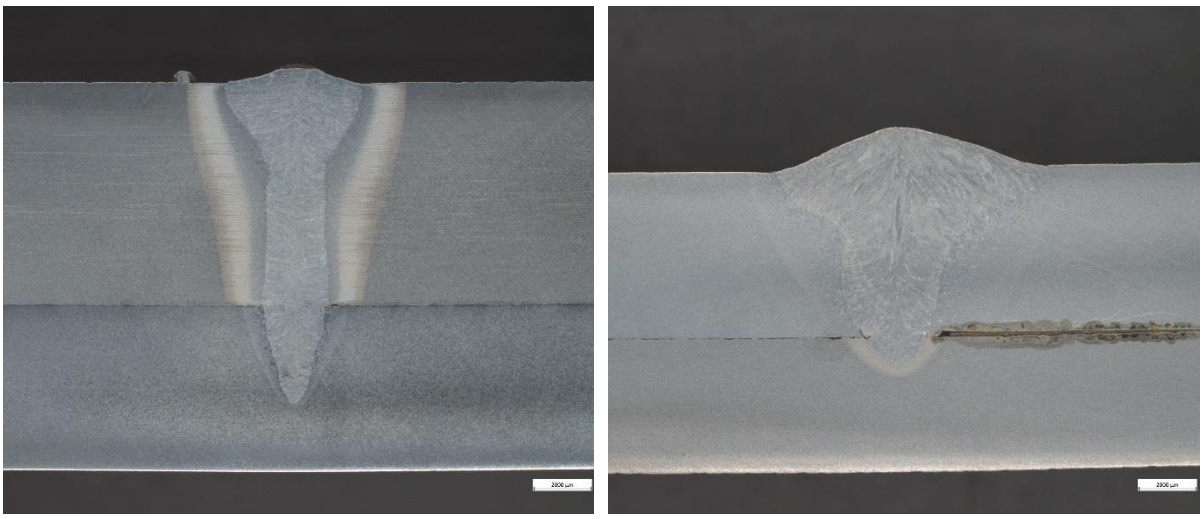

a) b)

Figure 7. Microscopic images from stake-weld cross section; a) pure laser, b) hybrid laser-arc.

A continuous corrugated core can be produced in two ways, either by multiple single-wave channels joined together, or a single plate with several corrugations, see Figure 8. The single-wave channels need to be joined into a continuous core plate with a width equal to the panel width. For the core-to-core welds, where two unprepared plate sides are joined, a hybrid laser-arc weld is more suitable than a pure laser weld due to its capacity of filling the gaps and handling tolerances. Core-to-core welds are also needed for the case of continuous core plates (Figure 8a) if the maximum width with respect to production of the corrugated plate is less than the final panel width.

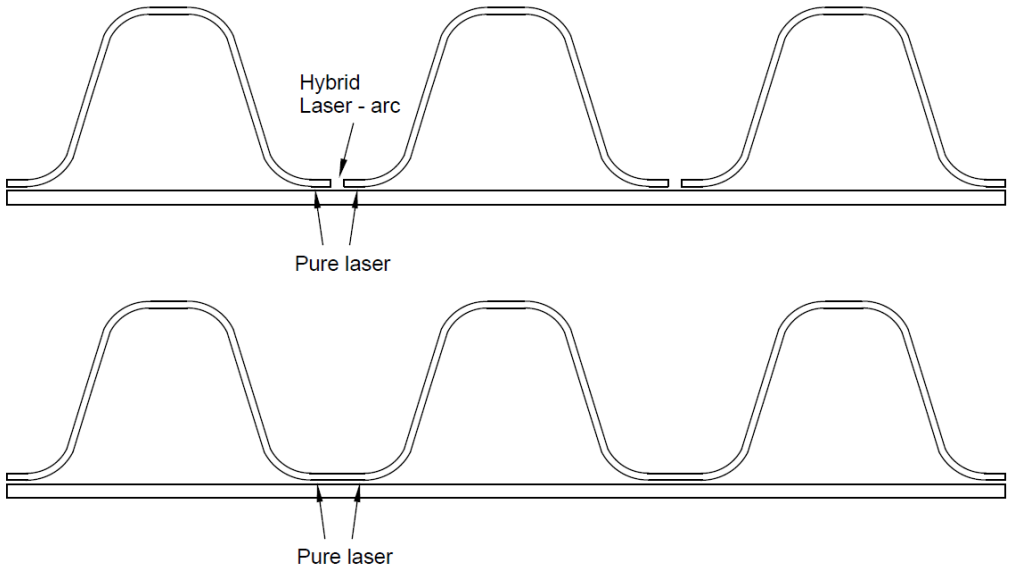

a)

b)

Figure 8. Two ways of manufacturing the continuous core; a) multiple single-wave channels (continuity is created by hybrid laser-arc), and b) continuous cold-formed core plate [Paper I].

When a pure laser stake weld is performed, good contact between the core and the face plates is of high importance for obtaining good weld geometry. Due to this aspect, a clamping-system is needed, see Figure 9 for the clamping system used in the manufacturing process presented in Paper I. Furthermore, in order to reduce the gap during production high demands on tolerances of the core shape are needed. A too large plate gap can impose a miss-shape of the weld, see Figure 10. The geometric miss-shape of the weld lead to a stress concentration at the intersection between the weld and the plate, and will likely lead to a reduced fatigue life. Furthermore, it can also lead to a reduced depth of penetration that also can affect the fatigue life.

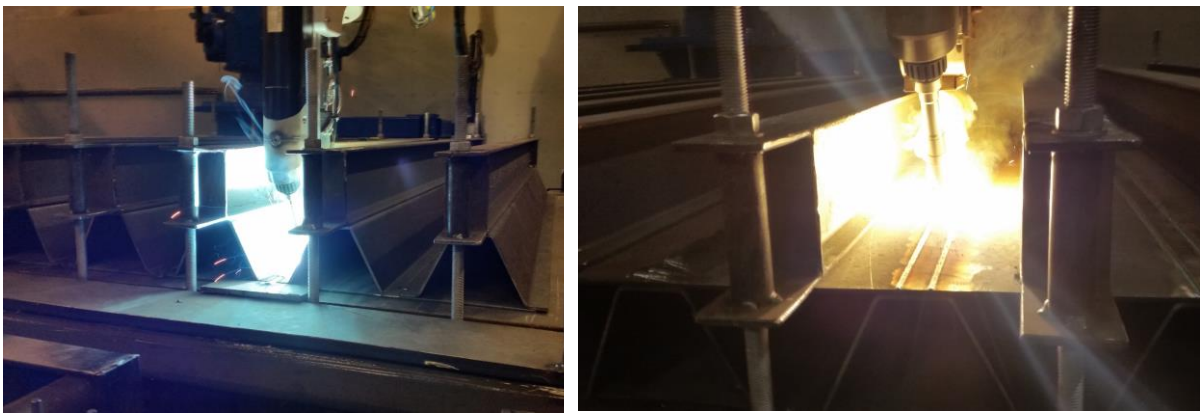

a) b)

Figure 9. Clamping for welding; a) bottom face joint [Paper I], b) top face joint, photo: Kleven Verft AS.

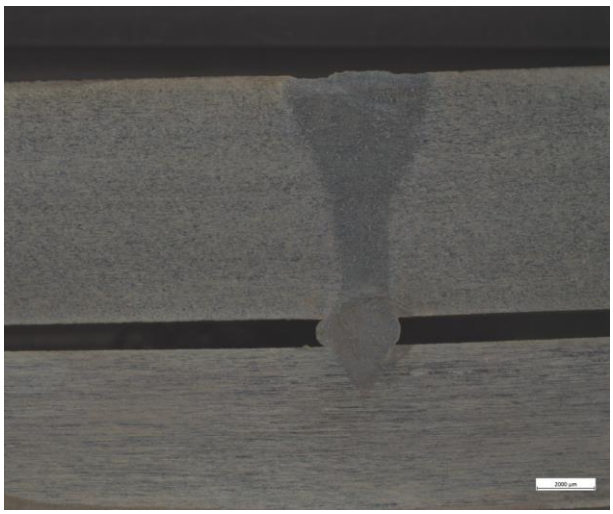

Figure 10. Miss-shaped weld due to large plate gap.

Figure 11 shows the cross-sectional geometric properties of a corrugated core steel sandwich panel with dual weld-lines. The penetration depth of the laser welding process determines the maximum thicknesses that can be used in the core and face plates. In Socha et al. [48], a laser stake-weld through a 16 mm plate is reported. Furthermore, when welding of the first side (e.g. core-to-bottom face joints) is performed, it can be executed from inside of the core and in to the face plate. In such a case, the size of the welding-head imposes limitations on the relations between *f, θ, h* and d_w of Figure 11.

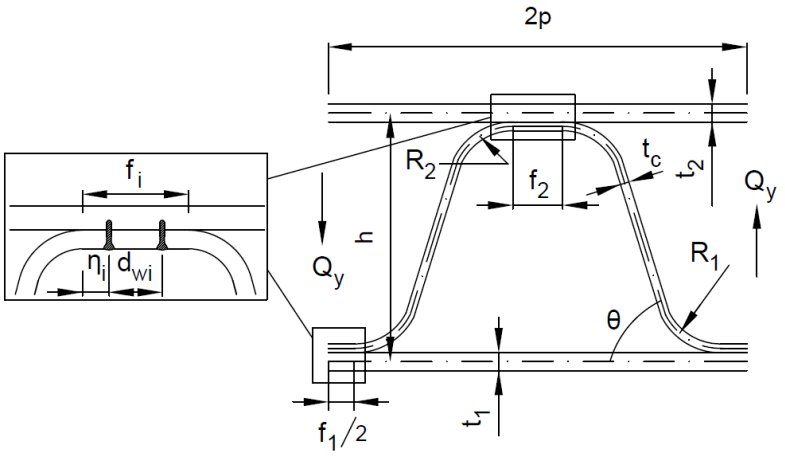

Figure 11. Cross sectional geometric properties of a corrugated core sandwich panel with dual weld lines [Paper IV].

2.2 PRODUCTION VARIATIONS

The nature of welding induces a spread of the geometric properties of the core-to-face joint in laser-welded CCSSPs. Several conditions from the welding process affects the final geometry of the joint as clamping, welding speed, focus of the laser-beam etc. In CCSSPs three geometric properties of the core-to-face joint region are dependent on the production conditions; t_w, e_w and h_g, denoting the weld width, weld misalignment and the plate gap height between the top face and core, respectively, see Figure 12. In order to ensure functionality of a sandwich panel for its entire service life, the natural spread of the production-dependent parameters from the used manufacturing process need to be determined and the effect of the variation of the parameters needs to be known. This lead to production tolerances, and within the limitations of the tolerances, the effects on the state of stress needs to be incorporated either on the load or the resistance side in a design situation. Furthermore, the measurements indicate the quality of the produced panel in terms of its geometric properties. It is worth mentioning that the panels that are produced for this project are demonstrators, with a topology that is produced for the first time, and increased geometric quality is expected in a well-established production situation.

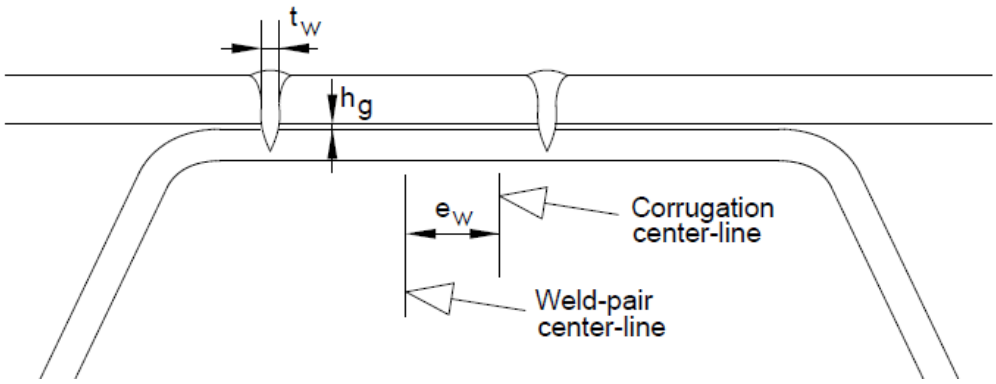

Figure 12. Joint region production-dependent geometric properties [Paper I].

In order to fulfil the aims related to the production of CCSSPs, four sandwich panels are manufactured, and the geometry of the core-to-face joint is quantified. The measurements, that are presented in Paper I, show that t_w varies between 1 and 4 mm and e_w is in 70% of the measurements equal to or less than 2mm. Regarding h_g, a larger scatter is identified. In the cases where a badly shaped weld is identified it is often occurring together with a significant gap between the plates. Furthermore, this is also an aspect that impacts t_w. Another property that is measured, using 3D scanning, is the deformations from the welding procedure. Figure 13 shows the deformations, in the face plates, in the mid-section of one of the 2 x 2 m panels (y is the weak direction of the panel). The measurements show that the internal plate fields of the panel have minor deformations from welding. However, a rotational deformation of the outer cells of the panel is identified. This rotational deformation yields a curvature in the weak direction of the panel. As an overall qualitative inspection of the quality of the panel in terms of geometric properties, good results are identified. However, the following aspects regarding observed geometrical deviations needs to be considered carefully in real production:

- contact between the plates during welding is needed in order to ensure proper geometry of the welds,
- miss-alignment between the core and the weld-pair is identified for some cases, care shall thus be taken to ensure proper alignment, and
- the overall curvature of the panel in the weak direction is significant, leading to the importance of further investigation/specification of welding sequence in order to reduce distortion from welding.

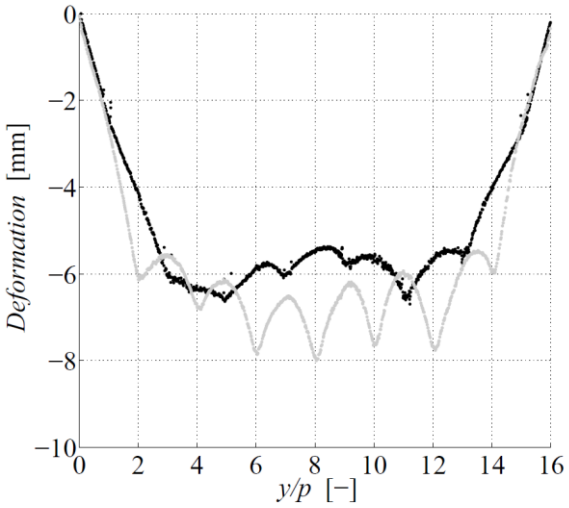

Figure 13. Face plate deformations of produced panel obtained from 3D scanning. Grey curve indicate measurement of the bottom face while the black curve show the top face. [Paper I].

The aim of the work that is related to the impact of production-related aspects is to determine if and to what degree are stresses in the weld region sensitive to the measured differences between the idealised and the real geometry. The measured variation of the geometric properties of the joints is used as a basis for a parametric study based on FEA. The focus of this parametric study is on load effects in the weak direction of a CCSSP, and therefore, a beam from a transverse section of a panel is studied. For the parametric study in Paper I, three different beams with two different sets of loads and boundary conditions are studied. Load cases 1 and 2 aim at isolating load effects of Directly Applied Load (DAL, global action is prevented) and pure global load effects, respectively. Furthermore, all models are executed both by including or excluding contact interaction between the face and core plates. Two normal stresses at the position of the welds (in the outermost fiber of the top face and the core) and the principal stresses in the weld notches are the chosen outputs of the study. The fatigue-relevant output stresses and their corresponding crack modes are shown in Figure 14. Based on the measured joint region geometries, three levels for each of the three parameters are included in the parametric study: [1 mm, 2.5 mm, 4 mm], [-2 mm, 0, 2 mm] and [1 μm, 50 μm, 100 μm] for; t_w, e_w and h_g, respectively. This parametric study includes the result of 324 2-dimensional (2D) continuum element FEAs.

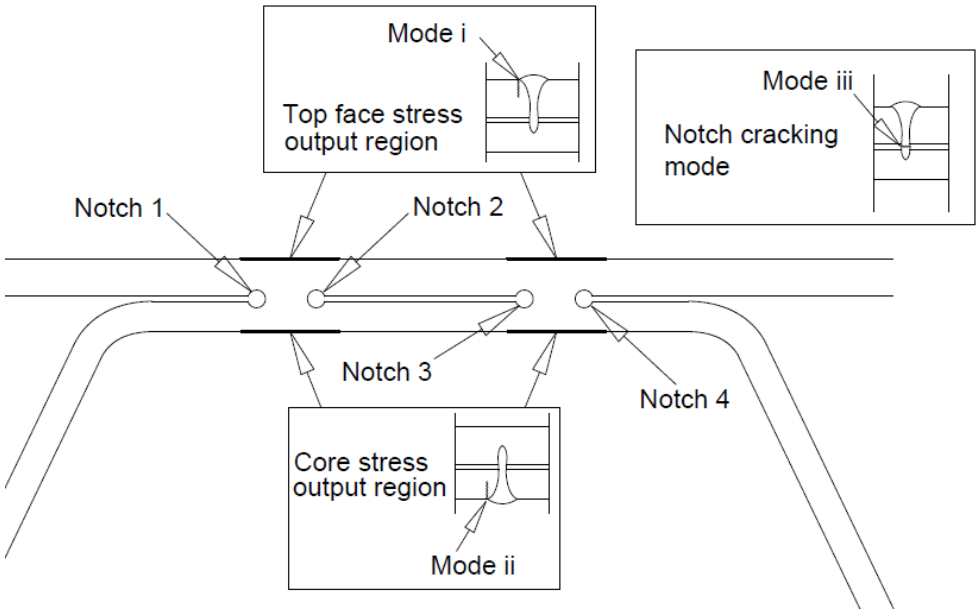

Figure 14. Fatigue-relevant output stresses of the parametric study and their corresponding crack-modes [Paper I].

The results – for the three investigated cases – show that weld misalignment has a modest impact on the top face normal stresses. However, the impact on the notch and core stresses is shown to be significant. Considering isolated global load effects, a weld misalignment of 2 mm can yield up to a 40% increase in notch stress. Weld misalignment has a more pronounced effect for the case of pure global load effects compared to the case of isolated local effect under directly applied load. The reason for the significant impact of the weld misalignment can be related to the high stiffness of the joint region. When the external load enforces unequal rotations of the two welds in a weld pair, restraint shear forces act on the welds, leading to high stresses in this region. Thus the tolerances with respect to this factor needs to be limited in production and accounted for in the design of CCSSPs

Considering the effect of weld width, the results of the parametric study show that this parameter has a small effect on the top face and core normal stresses in the vicinity of the weld. However, change in weld width was found to have a considerable effect on the notch stresses. Furthermore, the results show that an increase in the weld width can both increase and decrease the notch stress. This may be due to the fact that increasing the weld width increases the core-to-face interaction simultaneously as the section modulus and area of the weld itself increases.

When contact interaction between the core and the face plate is excluded in the analysis, the plate gap has no or very modest impact on all investigated output stresses. However, when contact interaction is included in the analysis, the gap size has a major impact on all three investigated stresses. This is because the gap size is the main influencing factor for determining at which load-level contact between the core and face plates occur. For the load case with isolated effect of directly applied load, contact always decreases the fatigue-relevant stresses. However, for the case of pure global load effects, it is shown that contact interaction can also lead to increased stresses.

3 FATIGUE

In steel bridge decks, fatigue is a known cause for premature deterioration. The origin to fatigue failures in conventional OSDs is a combination of complex geometry and the direct contact with localised loads that cause flexure in the deck-plate. On an analogous basis, proper fatigue design is a key aspect for CCSSP bridge decks.

3.1 ASSESMENT METHODS

Regarding fatigue-assessment of welds, there are several different commonly adopted methods in both practical engineering and research context. The most common methodology for steel bridge design is the Nominal Stress (NS) approach. This method is widely used in practice as it is compatible with simplistic structural analysis models that are used for design purposes. The method is incorporated in most design codes as CEN [49] and Hobbacher [50]. Here, the geometry of the investigated detail, the local geometry at the location of the crack initiation point and the internal flaws in the weld material are incorporated on the resistance side. This leads to individual design strength curves for each joint type. Another assessment approach is the Effective Notch Stress (ENS) method. This method was first introduced by Radaj [51] where the joint geometry and the local geometry at the crack initiation point is included in the structural analysis. This leads to a flexible methodology that can handle complex geometries where the fatigue strength is defined by a single S-N curve. The ENS approach has been commonly used in bridge-related research (see e.g. Al-Emrani and Aygul [52]) and it is included in the design code [50]. However, the main drawback with this methodology is that it places high demands on the structural analysis; that needs to be performed with continuum elements (2D or 3D solids). In [50], two different reference radiuses are given for the ENS approach, r_{ref} = 1 mm and r_{ref} = 0.05 mm. In CCSSPs for bridge applications, plate thickness down to about 5 mm can be feasible. Using the r_{ref} = 1 mm in such a case has an effect on the stiffness of the plates locally, see Figure 15. For this reason, the use of r_{ref} = 0.05 mm yields a more versatile assessment approach. Related to the reference radius r_{ref} = 0.05 mm a fatigue strength $\Delta\sigma_C$ of 630 MPa and a slope coefficient m = 3 is given in [50]. The general application for the smaller reference radius is welds in thin plates (below 5 mm). For the application at hand, plates that are significantly thicker than 5 mm are relevant. However, Frank et al. [53] motivated the use of this smaller notch reference radius by considering the small weld width (measured to 1 – 4 mm, Paper I) as a structural part. Another methodology that can be used is to apply the J-integral as a fatigue-determinant parameter, see e.g. Lazzarin and Livieri [54]. One advantage with the J-integral approach is that it includes no "cut-out" of material, as is the case of the ENS approach, even though the impact is generally modest when the r_{ref} = 0.05 mm is adopted.

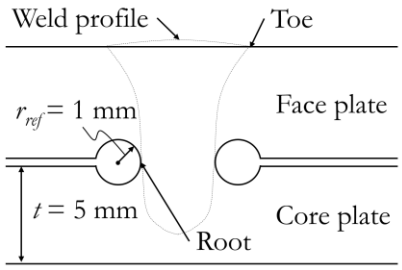

Figure 15. Effect of r_{ref} = 1 mm.

3.2 KNOWLEDGE GAP

For laser stake-welds, several authors has performed experimental work in order to investigate the fatigue strength (e.g. Frank et. al [53], [55]–[57], Fricke et al. [42], Ungermann and Russe [15], Bright and Smith [58] and Kozak [59]). A laser stake-weld fatigue crack can initiate from two positions; the weld toe or the weld root, see Figure 15. However, Kozak [59] showed that with respect to cracking from the toe, the fatigue strength is high. This leads to the conclusion that the more sensitive root crack initiation point is the relevant failure-mode for determination of the fatigue life of CCSSPs. In the above-mentioned references, web-core sandwich panels has been the target of investigation. For web-core sandwich panels, the laser stake-weld is performed on two plates that are oriented orthogonally to each other. Only Bright and Smith [58] has investigated fatigue failure of a stake-welds that joins two parallel plates. In [58] the outer face surface stresses were used as the fatigue parameter, and as no data regarding contact position and weld geometry was stated, these results are hard to compare to the other data that are given in terms of ENS. Thus, there exists no fatigue failure data that relates to laser-welds in two parallel plates, which is the case in CCSSPs. The fatigue tests that are performed by Fricke et al. [42] and Frank et al. [53] on laser-welded web-core T-joints, has only a few data-points above 1 million cycles to failure. Thus, more data in the low-cycle regime is of major interest. Furthermore, to the knowledge of the author, there exists no fatigue test-data regarding stake-welds in Duplex stainless steel.

3.3 EXPERIMENTAL DESIGN

At the sides of a weld in a CCSSP core-to-face joint, two principally different deformation modes can take place, contact or splitting action, see Figure 16. In the general case, independent of the type of action, the weld carries bending moment, axial force and shear force perpendicular to the weld direction. However, when contact action occur at one side of a studied weld (see Figure 16), the weld will be subjected to normal stress that mainly originate from axial force, compared to a weld that is subjected to splitting action where the bending moment in the weld is dominant (Figure 16). When a CCSSP is subjected to panel-level shear-force in the weak direction, the core-to-face joint will be subjected to splitting at one side of the joint, and contact action on the other side. Contact action occur in several other situations as e.g. in the top face under a patch load.

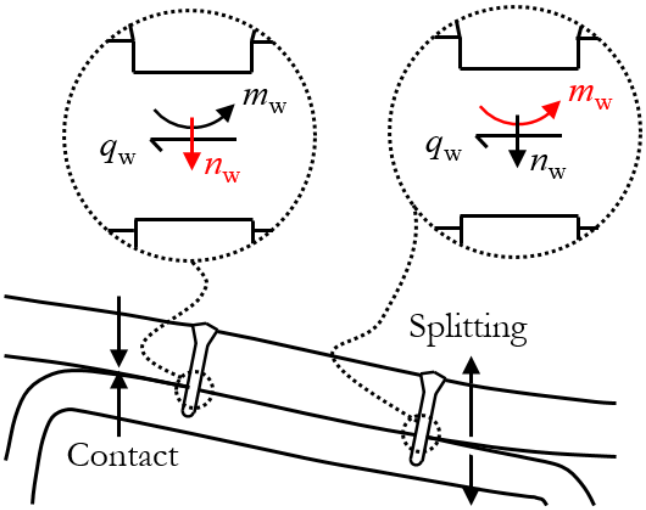

Figure 16. Contact and splitting action in corrugated core steel sandwich panels with dual weld lines.

In order to fill the knowledge gaps regarding the fatigue strength of laser-welds of CCSSPs, fatigue tests together with numerical analysis and assessment with both NS and the ENS are performed and the results are reported in Paper II. The fatigue tests are executed with cell-type specimens of CCSSPs, see Figure 17. Due to the two typical deformed shapes, two different Load Cases (LCs) are constructed for the fatigue-tests of cell-type specimens, see Figure 18. LC1 is constructed in such way that the decisive weld with respect to the fatigue life has contact action in its vicinity while the weld in LC2 has a splitting action. The number of tested specimens that are made of conventional C-Mn structural steel S355 and Duplex stainless steel are 16 and 5, respectively. In addition to the cell-specimens, a panel-specimen is tested under static and cyclic loading. These tests are performed in order to investigate the fatigue-performance of a full panel on a larger scale. The test-setup for the panel-specimen is shown in Figure 19.

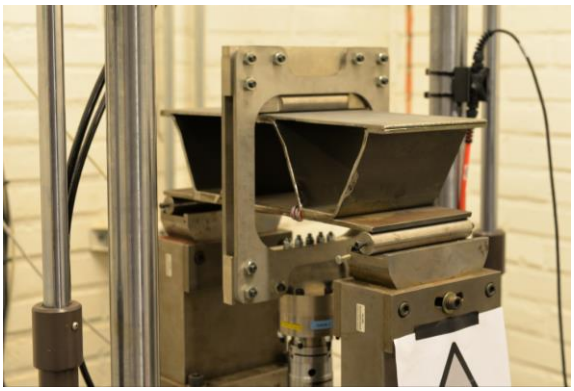

Figure 17. Fatigue test setup for cell specimens [Paper II]

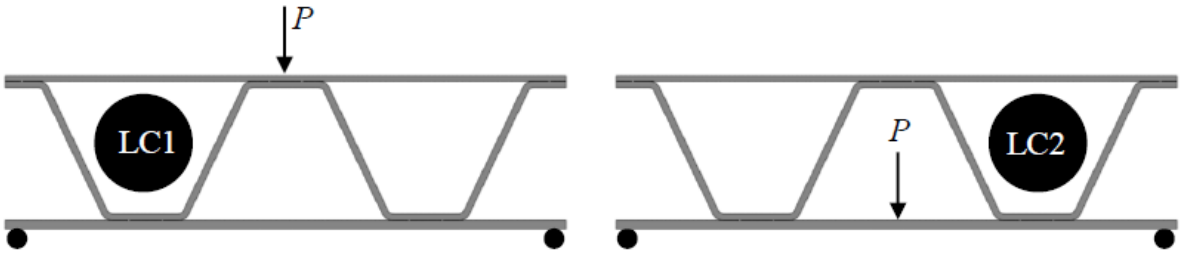

a) b)

Figure 18. Load-cases for fatigue tests of cell-specimens; a) LC1 and b) LC2 [Paper II]

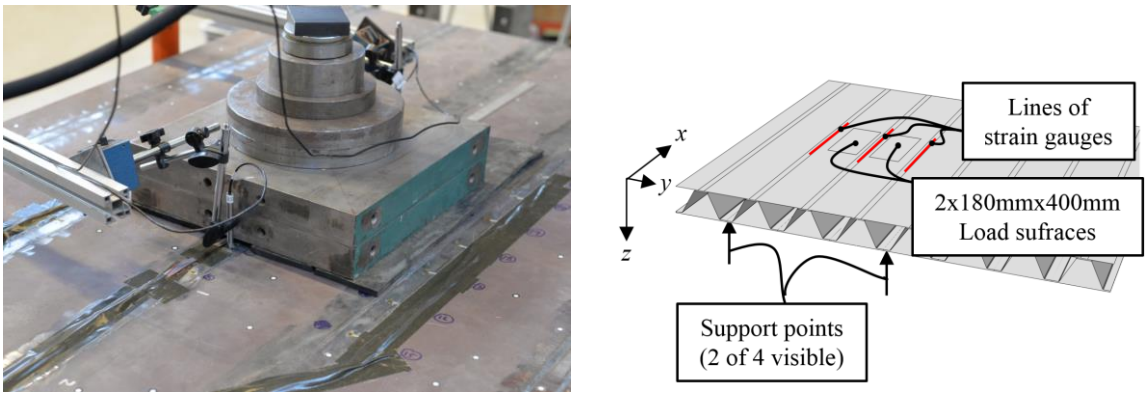

a) b)

Figure 19. Panel test setup; a) load application, b) schematic of load, support and strain gauges. [Paper II]

3.4 SUMMARY AND REMARKS

The test results that are presented in Paper II show that for LC1, fatigue failure took place through the weld. LC1 is the case in which the weld is subjected to predominant axial forces due to contact action between the face and core plate. Thus, the results are directly comparable to the results that are presented in [42] and [53]. In addition, the results that are presented in Paper II show that a crack-mode that initiates at the weld root and propagates through the base plate is possible in CCSSPs. This crack-mode is observed for all specimens loaded according to LC2; with a splitting action at the side of the failing weld. Crack-propagation through the core has not been observed in any of the fatigue tests that are presented in the literature. The crack-mode occur when the weld is exposed to splitting action that cause a bending action also in the face and core plate in the direct vicinity of the weld, see the failed specimens and the corresponding stress distributions of both the welds and core plate for the two crack modes in *Figure* 20.

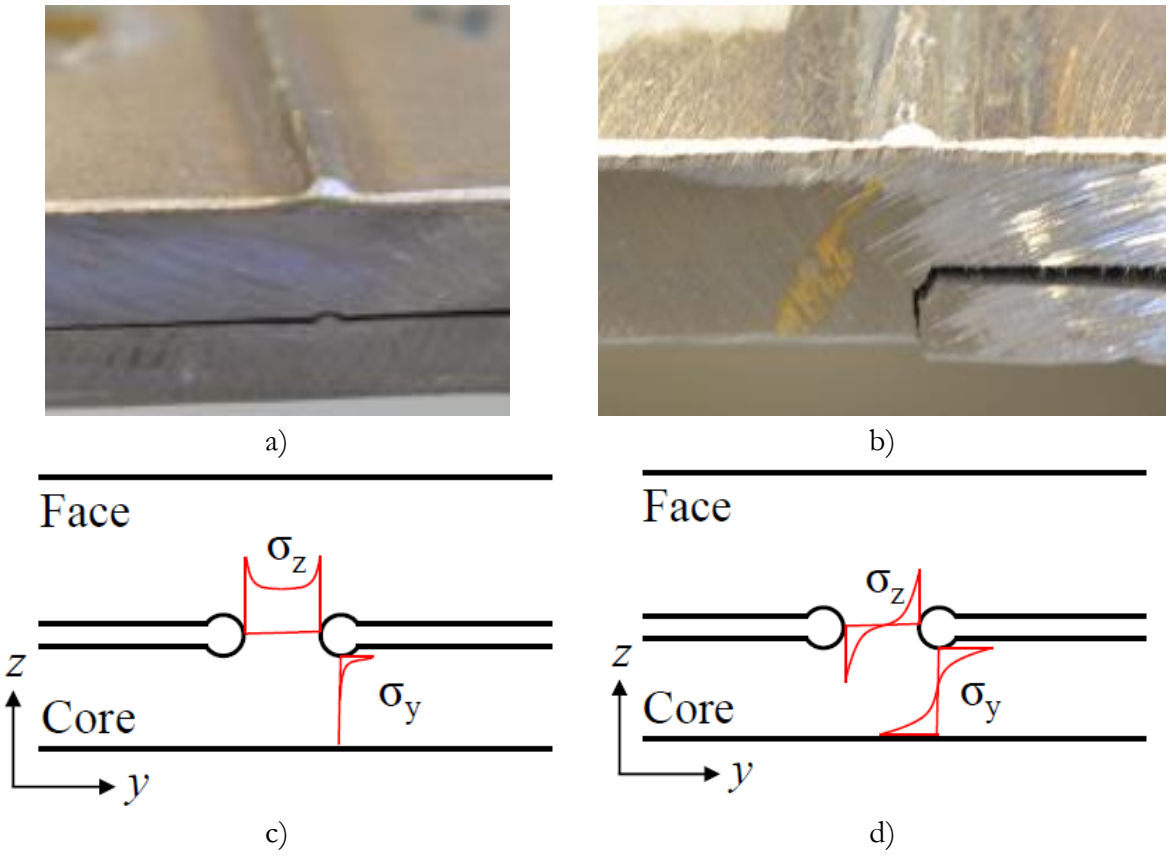

Figure 20. Photo of fractured part, a) weld-crack (LC1), b) core crack (LC2) and principal stress distributions for c) LC1, d) LC1 [Paper II].

A general conclusion from the work presented in Paper II, considering ENS as the fatigue parameter, is that independent of LC and crack-mode of the performed tests, the results are in alignment with the existing fatigue test data that are available on web-core T-joints. Including all the relevant test-data in the literature and the tests performed in Paper II, it is shown that using the fatigue strength $\Delta\sigma_C$ of 630 MPa and a slope coefficient m = 3 (recommendation in design code [50]) is slightly non-conservative ($\Delta\sigma_C$ = 580 MPa with fixed slope m = 3, see Figure 21). However, if the test-data below 10^4 cycles to failure is removed due to its irrelevance for bridge applications, the recommendation is slightly conservative instead. The natural slope of the test data is more shallow (m = 4.0) and the characteristic fatigue strength related to the natural slope is higher ($\Delta\sigma_C$ = 825 MPa) than the given recommendations. Thus, for a design situation, the current recommendation is valid, with a restriction for load-effects in the high stress-range. Alternatively, the design recommendations can be updated for laser stake-welds, in order to utilise the capacity of the weld better and gain more material-efficient structures, by having a larger characteristic fatigue strength together with a larger slope. However, updating the existing recommendation for a specific detail opposes the fundamental efficiency of the ENS approach that origins from a limited number of S-N curves. Another aspect that is visible in the test data that is shown in Paper II is that the natural slope varies between the two different load cases. Thus, the natural slope is shallower in LC1, with a crack-mode that propagates through the weld, compared to the propagation through the base-plate in LC2. Frank et al. [53] identified a possible cause for the shallower slope in their test results (compared to conventional welded

joints) as the failure propagation through the weld, in which the material properties are fundamentally different in micro-structure compared to the base-plate metal. The identified difference in slope between LC1 and LC2, supports this statement in [53].

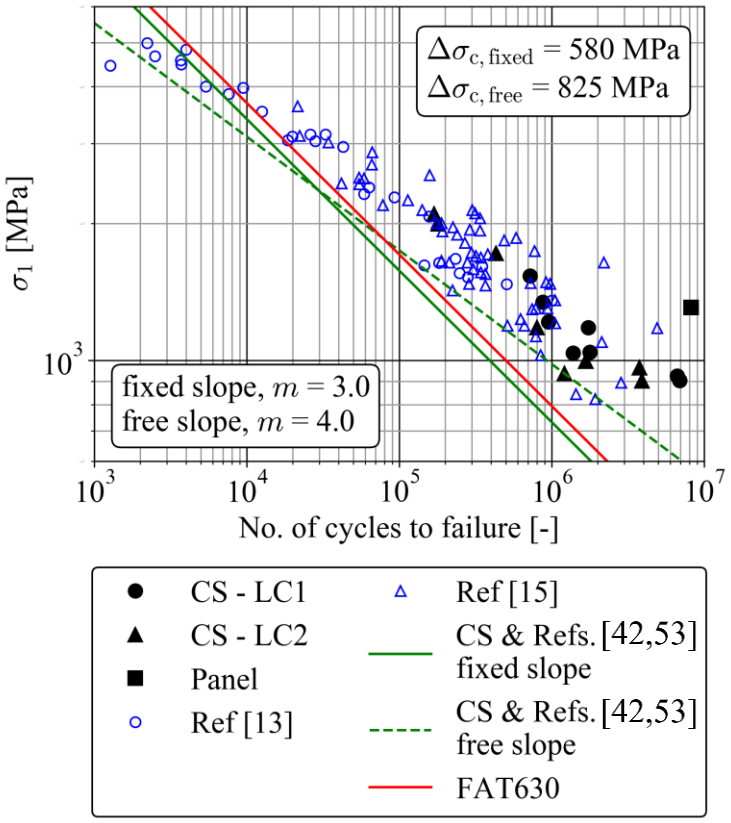

Figure 21. Fatigue test data from the literature and present fatigue tests [Paper II].

In Paper II, the fatigue strength with NS as the fatigue parameter is also investigated. In this analysis a beam element model together with spring elements for incorporation of the weld region rotational stiffness (see Paper V) is used for the stress determination. With respect to the NS approach, the two crack-modes needs to be investigated separately. Considering test data from [53] (pure axial force and crack-propagation through the weld) together with the test data from LC1 a characteristic fatigue strength of 57 MPa is derived on the basis of a constant slope m = 3. Again, the natural slope coefficient yields a more shallow inclination of the S-N curve and a higher characteristic fatigue strength.

The results from the test specimens that are loaded according to LC2 showed a modestly higher fatigue strength compared to LC1. As there exists no other tests in the literature with respect to fatigue cracking through the base-plate, the amount of data points is limited. All the data points are in the range between 10^5 and 10^7 in term of number of cycles to failure. Further investigations are to that end needed in the context of crack-propagation through the base metal. However, the test results given in Paper II show a higher characteristic fatigue strength implying that the same fatigue strength for the two crack-modes can be used as a conservative assumption. This determination of the fatigue strength in terms of NS opens for fatigue design using structural elements (beams and shells), on the condition that these

can capture the real behaviour of the structure to a satisfactory level of accuracy. This aspect is treated in Section 5.

For several bridge applications, Stainless Steel (SS) solutions are gaining market shares due to its reduced need for maintenance activities. However, the stainless structural steels are more expensive than conventional C-Mn Steels (CS). Considering these aspects; lightweight solutions are highly relevant for the use of stainless steels. In Paper II, the fatigue strength of CCSSPs with SS is investigated and the results show that the fatigue strength is considerably higher compared to the CS test specimens. However, only 5 data-points were collected making the statistical determination questionable.

Another aspect that has been considered for both web-core sandwich panels and CCSSPs is to fill the cell voids with a structural lightweight material, such as polymeric foam, see Gunecha [60] considering CCSSPs and Frank et al. [61] for web-core sandwich panels. Both these references show that filling the voids has a major effect on increasing the fatigue-performance of the panels. The enhanced fatigue-performance is the result of a considerable decrease in the weld stresses when the core material provides support for the constituent plates of the panels cross-section. However, this addition to the structure increases the panels complexity both with respect to load-carrying behaviour and manufacturing and the amount of research in this respect is limited. Another aspect that can be questioned is the economic and environmental effect with respect to both material consumption and manufacturing. Thus, there is a need for further investigations regarding this - highly relevant – addition to the structure.

4 STRUCTURAL ANALYSIS

4.1 INTRODUCTION

At present there exists no well-established and verified analysis methodology that directly can be applied in the design of CCSSPs that are a part of a structural system (e.g. a CCSSP supported by longitudinal and transversal girders). Such a methodology needs to be able to predict the average deformations of the panel and stresses in all the constituent members of the cross section, including the welds. One possible methodology that is often adopted in the design of complex steel structures is to use 3D shell element models. This is a possibility also for CCSSPs. However, validation of this concept is needed. In the work presented in this thesis, a model that incorporates 3D continuum elements (solids) is utilised for the verification of the 3D shell element analysis. The main challenge regarding the accuracy of the 3D shell element model is related to the modelling of the weld region and the connections to the supporting load-carrying structure.

Even though it can be possible to perform 3D shell element analysis, this is a computationally heavy duty. This is due to the many separated plate fields that need a specific number of elements in order for the deformations to be adequately resolved and thereby yield the correct stiffness properties of the panel and accurate stress predictions in all the constituent members of the cross-section. Thus, the numerical system is large and in design and optimisation situations; a considerable number of iterations are needed. This indicates the need for a simplified methodology. One computational technique that is often utilised for the simplification of panel structures is homogenisation. This technique utilises the panel's equivalent stiffness properties in order to simplify the 3D structure into a 2D Equivalent Single Layer (ESL). Figure 22 shows principle figures of a 3D shell element and an ESL model. The structural analysis approaches that are investigated in this thesis rest on this technique, to varying extents. Furthermore, the weld region deformation is an important aspect for these panels, and this subject needs to be treated independently of the chosen structural analysis approach, if it incorporates structural elements.

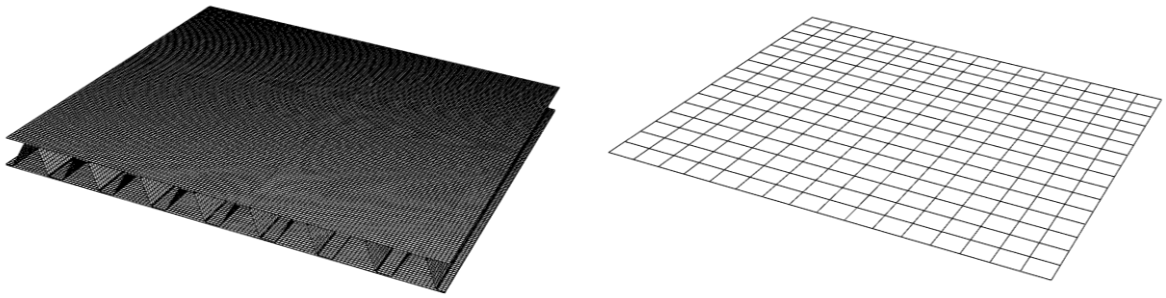

a) b)

Figure 22. Principal mesh sketch; a) 3D shell element model, and b) ESL.

4.2 MODELLING APPROACHES

In the work presented in this thesis, two different structural analysis methodologies for laser-welded sandwich decks are considered. First, a deformation-driven *sub-modelling approach* is considered for the design of CCSSPs. The sub-modelling approach is a multi-level analysis approach where the first level of analysis considers the full structure, a global model with a low detail level. In the analyses that are performed within this work, the global model uses an orthotropic ESL deck. A second level comprises a more detailed analysis which is performed on the region of interest. The second level (local) model is driven by the deformations obtained from the first level (global) model, see Figure 23.

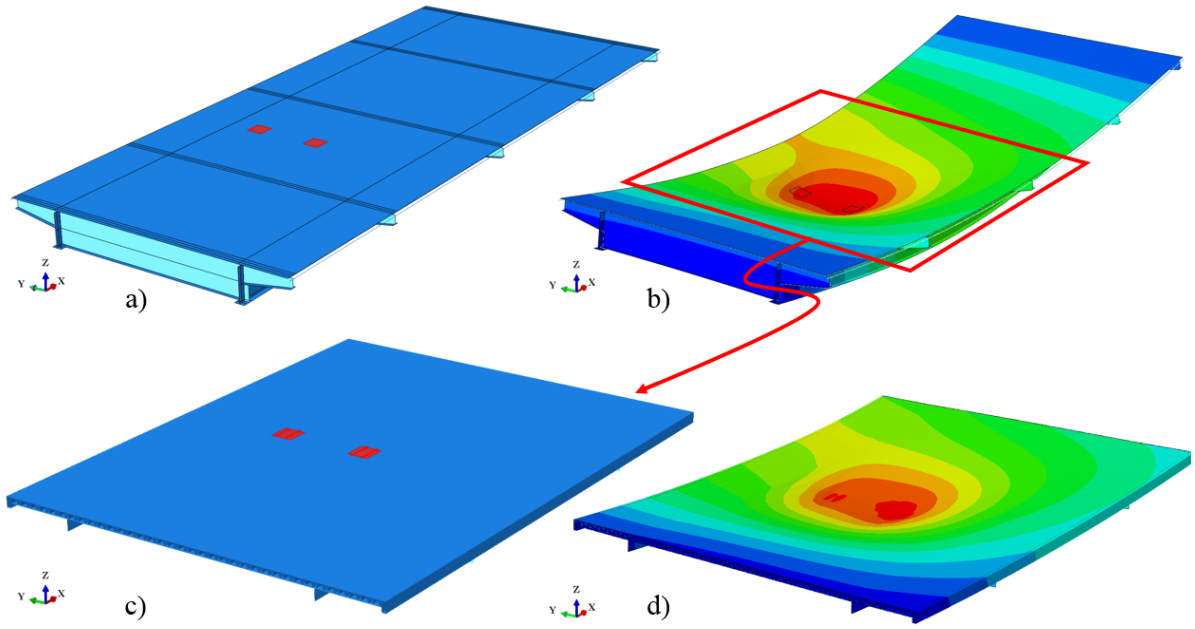

Figure 23. Principle sketch of sub-model approach; a) Level 1 undeformed (red highlighted regions are patch loads), b) Level 1 deformed, deformations in the highlighted region are used as boundary condition for Level 2, c) Level 2 undeformed (red highlighted regions are patch loads), and d) Level 2 deformed shape.

The second methodology that is investigated in this thesis, rests to a major extent on the ESL analysis and is herein thereby denoted as the *ESL approach*. The principle steps of this methodology are shown in Figure 24. An advantage of this methodology is the short calculation time. In this approach, the effective stiffness properties are first calculated and used in the ESL analysis (Figure 24a and b), i.e. in a similar manner to the first step in the sub-modelling approach. Then the sectional forces from the ESL analysis are used together with the effective stiffness definitions to determine the stresses in the constituent members of the cross section from the panel-level sectional forces (Figure 24c). In this process, the discrete nature of the structure is lost. This has a major effect in regions of supports or DAL and it needs to be accounted for with a separate, decoupled, analysis (Figure 24d). This approach can also be applied to beams, with an analysis of a homogenised beam as a basis. For web-core sandwich beams and panels, all of the above-mentioned aspects were addressed by Romanoff et al. in [27], [62]–[66]. Buannic et al. [67] presented a numerical approach to

homogenisation methods covering the center-plane deformations of a general structural core sandwich plate but excluding the effect of directly applied load. He et al. [68] presented a homogenisation approach that follows the classical sandwich theory for global sectional force determination and used a simply supported continuous beam analogy for directly applied loads. However, to the author's knowledge, the homogenisation approach in conjunction with CCSSPs with dual-welded joints has not been addressed in the literature.

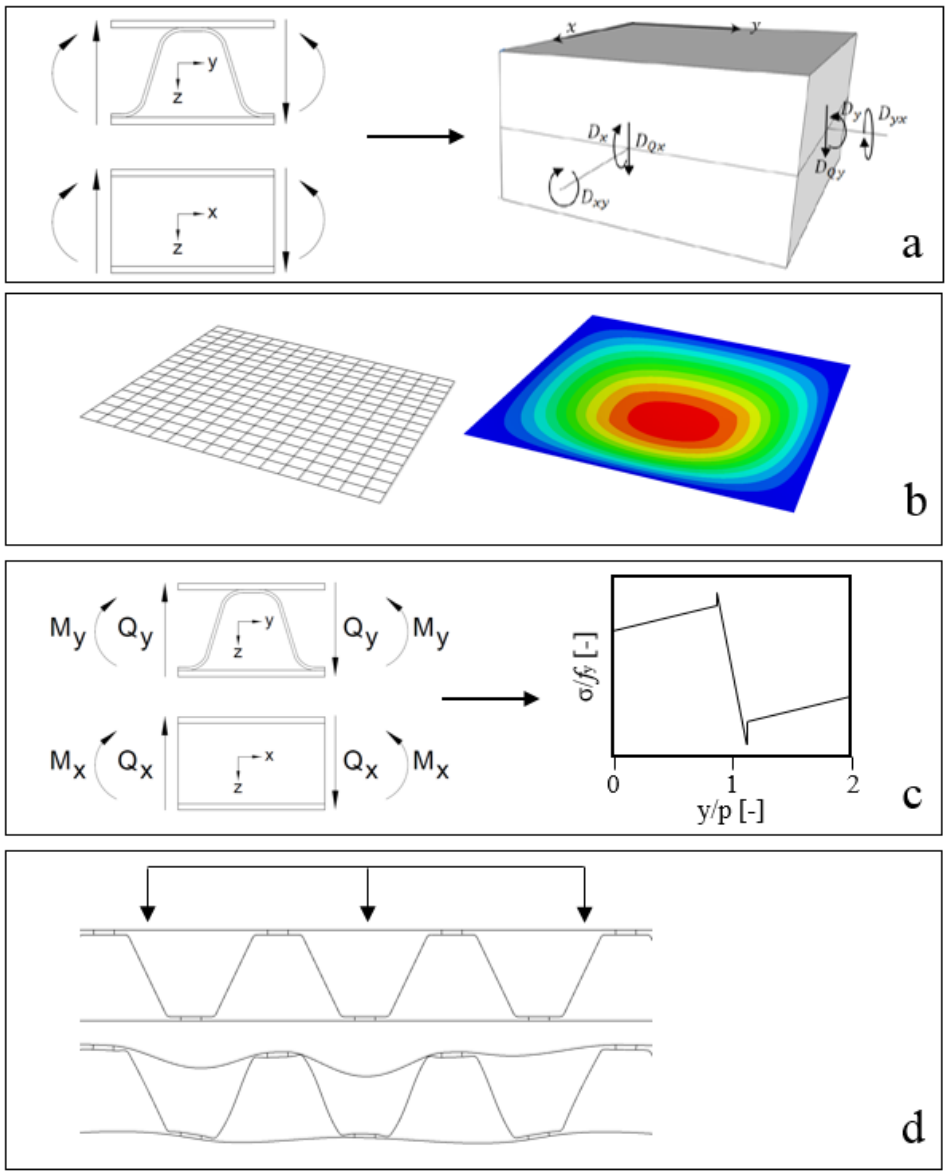

Figure 24. Schematic view of the ESL approach; a) derivation of equivalent stiffness properties, b) analysis of ESL, c) panel-level sectional forces causing local plate deformations yielding stress distribution in the constituent members of the cross section, and d) effect of directly applied loads (DAL) [Paper III].

There also exist other, more advanced approaches as the *coupled stress approach* (see Goncalves and Romanoff [69]) or the *micropolar panel approach* (see Karttunen et al. [46], [47], [70]). However, these approaches are developed for web-core sandwich panels and are not verified for incorporation of connection to supporting structures. For that reason, this third

category of more advanced approaches are not evaluated in the work that is presented in this thesis. Here the focus is directed towards the ESL and the sub-modelling approaches. Details on the investigated methodologies are given in Paper III. Another, numerical strategy, that can be adopted is the use of super-elements (or sub-structures), that aims to reduce the size of the numerical system by identifying different parts with identical geometry and external loading, as is described by Minnicino and Hopkins [71]. However, if this technique is to be used, the basic assumption of using 3D shells for CCSSPs needs to be verified.

4.3 SANDWICH PLATE THEORY

In the general case, a sandwich panel consists of two stiff face layers, separated by a core material, see Figure 25. All three layers are in general homogenous, but not necessarily isotropic. The faces carry bending moment while the core carries the shear forces. As the core material is in general lightweight and less stiff, the plate theory for sandwich panels need to account for shear deformations.

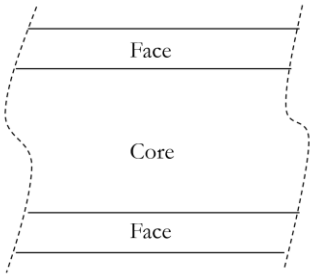

Figure 25. Sandwich cross section with homogenous layers.

The overall structural behaviour of homogenous sandwich plates including bending, stability, dynamic characteristics, etc., has been collected in several textbooks; see e.g. Allen [72], Plantema [73], Vinson [74], Reddy [75] and Zenkert [33]. Literature review regarding a wide variety of sandwich plate theories was presented by Noor et al. [76], and Vinson [77].

For the case of an orthotropic homogenous sandwich plate subjected to out-of-plane loads, defined by seven equivalent stiffness properties (two for bending, two for shear, twisting and two Poisson ratios), Libove and Batdorf [78] derived a small deflection theory following the well-known Reissner-Mindlin kinematics (see Reissner [79] and Mindlin [80]). The plate theory derived in [78] includes the transverse shear deformation contribution to the total out-of-plane deformation, and it was later extended to include curved sandwich panels by Stein and Mayer [81]. These first-order shear deformation theories (FSDT, i.e. linear distribution of in-plane deformations through the plate thickness yielding a constant shear strain distribution) are in the literature often referred to as classical sandwich theory. Another approach to sandwich plate analysis is the ABD-matrix approach or general sandwich approach for anisotropic plates, which is an extension of classical lamina theory (see e.g. Vinson [74] or Reddy [75]). The ABD-matrix approach includes the B-matrix that enables coupling of the in-plane and bending actions, i.e. including the effect of diverging neutral- and loading-plane (see e.g. Zenkert [33]). For CCSSP, the B-matrix is a null-matrix if the cross section is symmetric and a panel analysed by the classical sandwich theory and the ABD-matrix approach will be equivalent if FSDT is adopted. If significant discrepancies

with respect to the position of the neutral layer exist between the two orthogonal directions, excluding bending and membrane interaction can lead to considerable errors. Good agreement of the averaged response of CCSSPs has been reported in the literature using classical sandwich plate theory and full 3D numerical analysis or experimental analysis, see e.g. Dackman and Ek [14], Tan et al. [21] and Chang et al. [82].

Common for most sandwich plate theories is the assumption of thin faces, i.e. the faces act as membranes. An effect of this assumption is that the out-of-plane deformation from transverse shear has a singular derivative at discrete force application positions. The effect of thick faces at concentrated forces in sandwich beams with a homogenous core was addressed by Allen [72] and it was further explained in detail by O'Conner [83]. The thick face effect is likely to affect the results in CCSSPs for bridge applications close to supports if the support line and the corrugation direction is parallel. However, this topic is not addressed in detail in this thesis (even though it is briefly mentioned and visualised in Paper III). For 3D shell element analyses, the thick face effect is directly incorporated in the analysis.

4.4 CROSS-SECTIONAL PROPERTIES

The cross-sectional properties of a sandwich cross section are needed when considering homogenisation of a structural core sandwich panel into an ESL. Furthermore, a proper analytical derivation of a cross sectional property will together with the corresponding panel-level sectional force enable the calculation of the nominal stress distribution within the cross section in all of its constituent members, i.e. for the ESL approach. Cross sectional properties are defined in the literature for different types of steel sandwich cross sections. Common for structural core sandwich panels is that the stiffness properties are straight forward to derive, with exception of the transverse shear stiffness in the weak direction.

In 1950, Holmberg [84] published the derivation of the transverse shear stiffness for web-core sandwich beams. Lok et al. [85] presented a further developed derivation of the web-core transverse shear stiffness. Kujala and Klanac [86] introduced an expression for non-uniform web-core cross sections. Furthermore, Romanoff et al. [63] enhanced the definition of the transverse shear stiffness by incorporating the rotational stiffness of the weld region in the core-to-face plate connection.

For corrugated core sandwich cross-sections, Libove and Hubka [20] derived analytical expressions for all cross sectional constants, both with respect to in-plane and out-of-plane loading. For the transverse shear stiffness in the direction perpendicular to the core (see Figure 26), this work was performed using Euler-Bernoulli beam theory and a single rigid connection between the face-plates and the core. When the global transverse shear force is known from the homogenous beam or plate analysis, all local sectional forces of the constituent members of the cross section can be calculated using the derivation of Libove and Hubka [20]. Furthermore, Nordstrand [87] derived the shear stiffness in the weak direction, also using a single rigid connection between the face-plates and the core, but extending the theory of Libove and Hubka [20] to include curved beam theory according to Timoschenko [88]. However, in Nordstrand [87], only symmetric cross sections were considered. Atashipour and Al-Emrani [89] derived a transverse shear model in the weak

direction that include the shear deformations of the constituent members of the cross section and composite material properties. The derivations of Nordstrand [87], Libove and Hubka [20] and Atashipour and Al-Emrani [89] were performed using a single rigid connection between the face-plates and the core, and to the authors knowledge, no model that includes dual connection lines between the core and face plates exists in the literature.

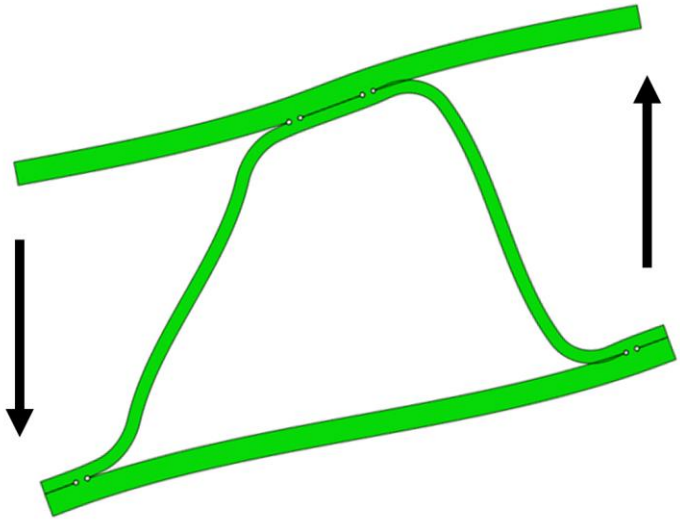

Figure 26. Transverse shear force in the weak direction, Qy.

Sandkvist and Palmgren [90], and Nilsson and Al-Emrani [13] showed that for bridge applications, the use of two weld lines between the core and the faces compared to a single weld line will lead to large decrease of stresses in the weld region, yielding an increased fatigue life and ultimate load-bearing capacity of the core-to-face joint. These analyses were performed without contact interaction between the core and the face plates. Furthermore, Persson [91], and Nilsson and Al-Emrani [13] showed that, implementation of a single rigid connection between the core and the face plates will lead to overestimations of the transverse shear stiffness in real sandwich plates. In fact, the response of the real structure will likely be in-between that of a model with a hinge and a rotationally rigid core-to-face interaction. Furthermore, with respect to laser-welded web-core sandwich panels, the influence of including the rotational rigidity of the weld region on the stress prediction was shown by Romanoff and Kujala [63]. In a corrugated core steel sandwich panel with dual weld lines, the slenderness ratio (length-to-thickness ratio) of the constituent members of the cross section may be small, i.e. less than 10. Thus, shear deformations in the constituent plates of the cross-section may affect the shear stiffness of the panel and the stress distribution within the cross section.

In Paper IV, a new model for the transverse shear stiffness in the weak direction for CCSSPs with dual weld connections at each core-to-face joint is presented. The analytical solution is based on the direct stiffness approach and it adopts the minimum potential energy theorem in order to compose the stiffness matrix for the non-straight core member. Timoshenko beam theory is adopted in the analytical model, i.e. the effect of shear deformations in the individual members are included. Furthermore, a rotational spring is

included in the analytical model in order to account for the rotational rigidity of the weld region. The accuracy of the analytical model for the transverse shear stiffness is to a large extent dependent on the degrees of freedom included in the model. A CCSSP half-cell under pure transverse shear is shown in Figure 27 together with the structural setup and the included degrees of freedom for the shear stiffness derivation. The results in Paper IV shows that the accuracy of the presented analytical model is high in comparison with 2D frame FEA, thus, the chosen degrees of freedom are adequate to represent the sandwich panel under pure shear. A closed-form solution for calculating the stiffness of the rotational spring is presented in Paper V.

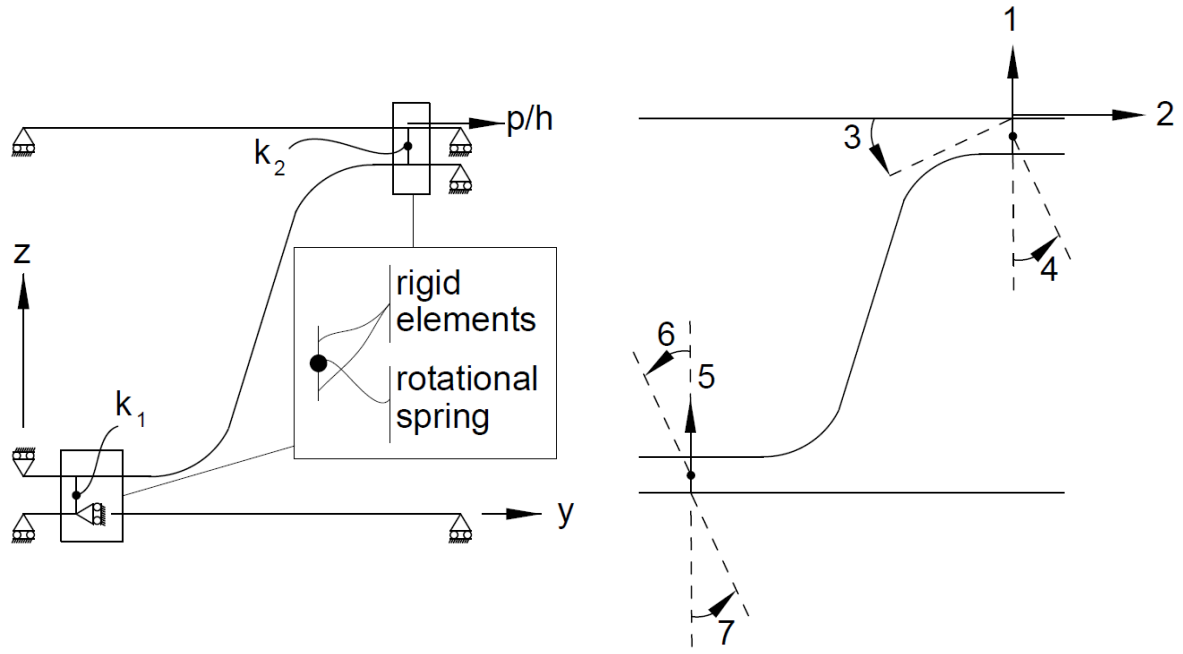

Figure 27. a) Structural setup for derivation of the transverse shear stiffness b) included degrees of freedom. [Paper IV].

In the analytical derivations that were presented by Libove and Hubka [20], the contribution to the stiffness regarding bending and membrane force in the weak direction from stretching of the core was neglected. However, depending on the cross-section geometry, this could lead to a significant error. For the analyses in Paper III, the weak direction membrane stiffness is analysed by a numerical model and it is shown that the stretching of the core increases the membrane stiffness in the weak direction by 2%. For future work, dependent on the cross-sectional configurations that shall be used in practice, it can be relevant to develop cross sectional properties for bending moment and membrane force in the weak direction for dual-welded CCSSPs. In such case, the methodology that is used in Paper IV can be adopted with a change in the load situation.

4.5 WELD REGION STIFFNESS

As previously mentioned, the welds of a CCSSP are a critical region, especially considering the fatigue performance of such plates. Furthermore, the weld is the element that connects

the core and the face plates and it has thereby an effect on the stiffness properties of the panel. Figure 28 shows a core-to-face joint region in a CCSSP. The joint region is in general complex considering stress prediction and has a significant rigidity. When structural elements (elements that exclude the thickness direction, i.e. shells or beams) are used in the analysis, the deformation that occur in the weld region needs to be accounted for as it effects the stiffness of the joint region and thereby also the load distribution within the joint. Thus, the nodes A and B (see Figure 28) are not rigidly connected. The main affecting weld deformation is the rotation, see Paper III. However, it is shown in Paper III that also deformations perpendicular to the weld-line (y-direction) and in the vertical direction (z-direction) can have a minor impact on the weld normal stresses, σ_z as they impact the joint stiffness.

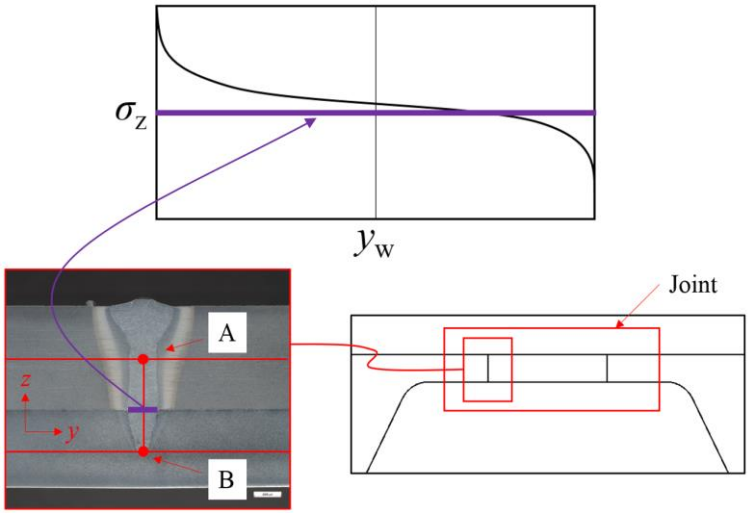

Figure 28. Core-to-face joint and weld region.

Modelling of the weld region stiffness in structural element models is in the work that is presented in this thesis performed using spring elements. In order to compare the weld stresses in the springs with those from solid element models, the nonlinear distribution of stress in the latter is linearised, and the nominal normal stresses originating from bending moment σ_{zM} and axial force in the weld σ_{zM} can be calculated (Figure 29). Figure 30 shows a schematic sketch of the modelling of a weld region for a 3D shell element model. Here, in addition to the deformations in y and z, the direction parallel to the weld-line (x-direction) is also included. Even though, the effect of this spring has not been investigated in detail, all relevant results in Paper III indicate that full rigidity in this direction is an adequate assumption. It is important that the location of the rotation occur at the correct position. For that reason, two stand-alone nodes are modelled with a small distance d between them (i.e. d is chosen as small as the numerical analysis tool admits), at the location where the two plates intersect. Each stand-alone node is coupled to the corresponding node in the core or face plate with a rigid connector, i.e. all degrees of freedom are connected.

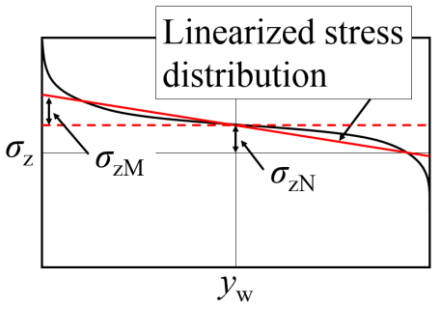

Figure 29. Calculation of nominal stresses from the stress distribution of the solid element model, [Paper III].

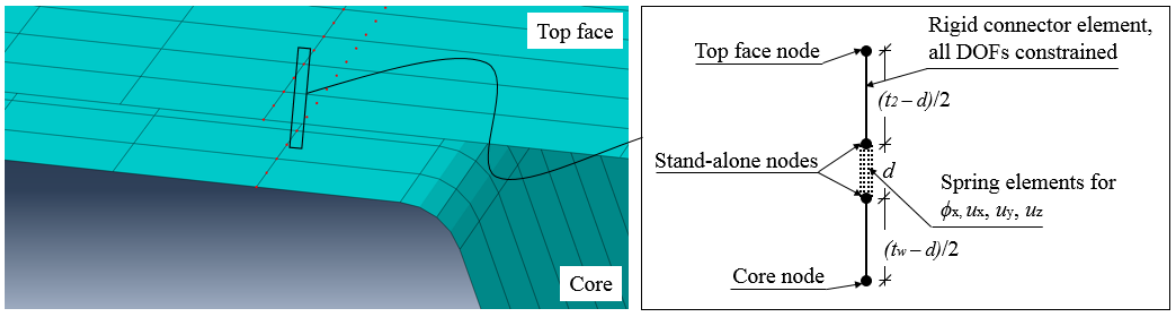

Figure 30. Modelling of weld region stiffness springs [Paper III].

As was previously stated, there is a need to incorporate the rotational deformation of the weld region both in the calculation of the elastic stiffness properties and in the 3D shell element analyses. Furthermore, it has been shown that it is the, by far, most important weld region deformation. In Paper V a closed form solution for the magnitude of the weld region rotational stiffness is presented. The solution is based on a large set of numerical analyses evaluated using regression analysis. Validation of the rotational spring model is made with respect to both 2D and 3D analysis. In Paper III, where the weld region deformations are studied, the spring stiffness components are calculated by numerical analyses, for the geometry of a single specific panel. Figure 31 shows the structural setup for calculation of each spring stiffness component.

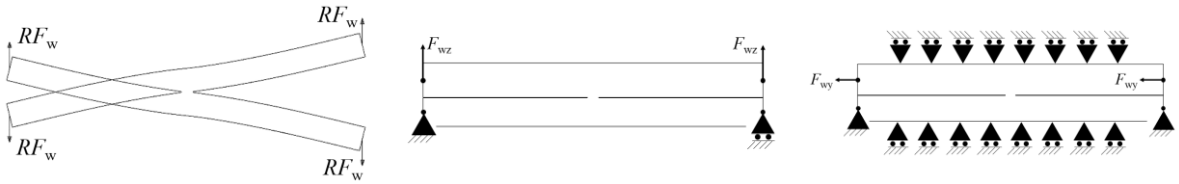

a) b) c)

Figure 31. Structural setups for calculation of spring stiffness components with respect to; a) rotational spring, b) z-direction spring (axial), and c) y-direction spring (perpendicular shear).

4.6 CORE-TO-FACE INTERACTION

One aspect that is highly relevant regarding structural analysis of CCSSPs, is the effect of contact action between the core and the face plates, see Figure 16. In general, contact action at the side of a weld causes a normal stress distribution, in the weld, which is dominated by axial force, while if no contact takes place bending will dominate the normal stress in the weld, see Paper II. In Paper I and II, the effect of contact is studied, and the results show that for all cases – except for a few cases (far from loads and supports) – excluding contact is a conservative assumption.

The reasons for lack of contact are; a gap between the core and the face or welding-induced deformation of the plates, see Figure 32 a and b, respectively. Both of these reasons are effects of the welding procedure. As the contact in general is beneficial, the initial contact needs to be verified for produced panels in order for it to be accounted for in design situations. In practice this is hard to achieve, and it is a topic in need of further research studies. As of now, the recommendation is to exclude contact action in design situations. However, if a load-situation of panel-level sectional forces alone is determinant for the design of a weld, analysis that include contact needs to be adopted.

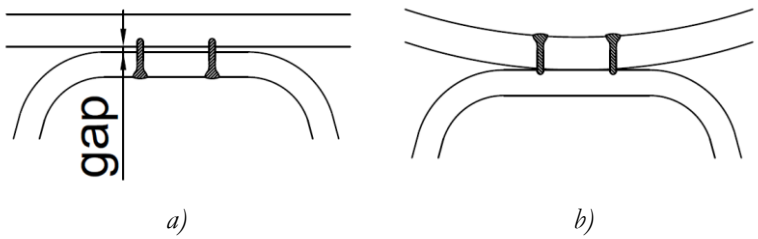

Figure 32. Sources for lack of plate interaction; a) gap, and b) welding deformation [Paper V].

Another aspect concerning the contact action between the core and the face plates is the position of the contact. The work that is presented in Paper II show that this is a parameter that has a significant effect on the stress magnitudes in the welds. However, detailed investigations in this aspect are left for future studies.

4.7 BEAMS

In Section 4.2, the ESL approach was introduced. Here, the special case of load distribution in the weak direction is studied, i.e. a strip (beam) from a CCSSP section. A case study is shown in this sub-section using the ESL approach. Thus, a methodology that adopts the ESL approach for beams to be valid for corrugated core cross-sections with dual weld-lines, subjected to panel-level sectional forces. Furthermore, the accuracy of this methodology is verified by numerical analysis and experimental results.

4.7.1 NUMERICAL ANALYSES

In this section, three different levels of structural analysis of a simply supported corrugated core steel sandwich beam are compared: (1) a 2D continuum element FEA, (2) a 2D frame FEA and (3) a one-dimensional (1D) analytical homogenised beam model. The geometric properties of the studied beam are shown in Table 1 and the notations are given in Figure

11. In this section the stresses in the outermost fibre of the top face, at a core-to-face joint with a clear distance from both loads and BCs are studied. Thus, the joint is subjected to panel-level sectional forces alone. All models in this case study are linear. The three compared models, the studied output area, loads and BCs are shown in Figure 33.

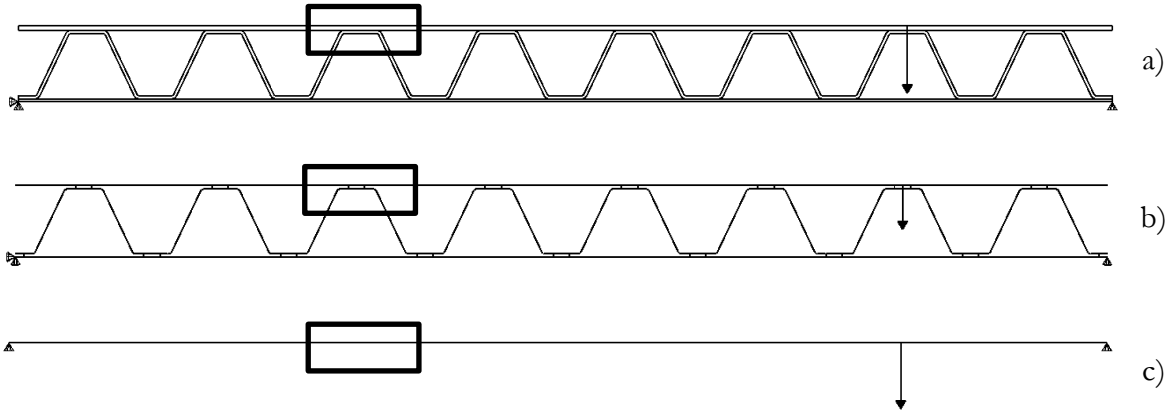

Figure 33. Three different levels of structural analysis; a) 2D solid element FEA, b) 2D beam element FEA, c) analytical homogenous beam analysis. The rectangular boxes indicate the investigated area/output region.

Table 1. Geometric properties for the case study beam.

t_1	t_c	t_2	h	θ	$f_{1,2}$	$d_{w1,2}$	$R_{1,2}$	$2p$	n_{cells}	t_w	b
[mm]	[mm]	[mm]	[mm]	[°]	[mm]	[mm]	[mm]	[mm]	[-]	[mm]	[mm]
5	6	8	132	64.4	60	30	7.4	253	8	1	190

For the analytical model, a homogenised beam is studied and the resulting sectional forces and moments are used to calculate the stresses in the constituent members of the beam. The top face stresses that originate from global shear action are calculated according to Paper IV and the results are compared with the model of Libove and Hubka [20]. The weld region rotational stiffness incorporated in this case study (both for the analytical and the 2D frame model) are determined according to Paper V as 18 kNm/rad. In the absence of an analytical model related to the panel-level bending, a 4-point bending numerical 2D frame model is used for the calculation, analogous to the calculations in Paper III. Furthermore, the linearisation approach that approximates the effect of non-constant sectional forces over a unit cell, which is shown in Paper III for panels, is also adopted here.

Figure 34a shows a comparison between the two 2D FEA models and the two analytical models where one uses a stress calculation from global shear according to Libove and Hubka [20] and the other adopts the model presented in Paper IV. Figure 34a shows that using the model of Libove and Hubka [20] for dual welded CCSSPs can lead to large errors considering stress predictions, which was expected. Figure 34a also shows that the two 2D FEA models are in perfect agreement, except at the position of the welds. In this region, there is a principle discrepancy between the two models where the continuum element model incorporates the distribution of the weld, and the frame model has discrete interaction points. Thus, stress predictions performed with a top face element, which lacks the ability to predict the correct

through-thickness stress distribution, will lead to conservative results. Figure 34a also shows that the analytical model that uses the shear model that is presented in Paper IV is in perfect agreement with the frame model. This validates the ESL-approach for stress predictions in CCSSP beams that are subjected to panel-level sectional forces if;

- the linearisation method for non-constant sectional forces is used (see Paper III),
- models regarding stress-predictions from the panel-level sectional forces that are specific for dual-welded CCSSPs are used (se Paper III and Paper IV) and
- the weld region deformability is taken into account (see Paper V)

Figure 34b shows the top face stresses for two special cases of the FEA frame model; one where the weld region rotational stiffness is assumed to be zero (hinge) and one where full rotational interaction between the core and the face plates is assumed (rotationally fixed). The stresses in the span between the joints show a modest discrepancy between the two cases. However, at and between the welds, a major discrepancy is shown. Thus, force transfer between the core and the faces – i.e. the nominal state of stress in the weld – is highly dependent on the rotational spring. In fact, in this special case, the nominal normal stress in the weld is increased with 75% for the case with a fixed connection compared to the model with a hinge.

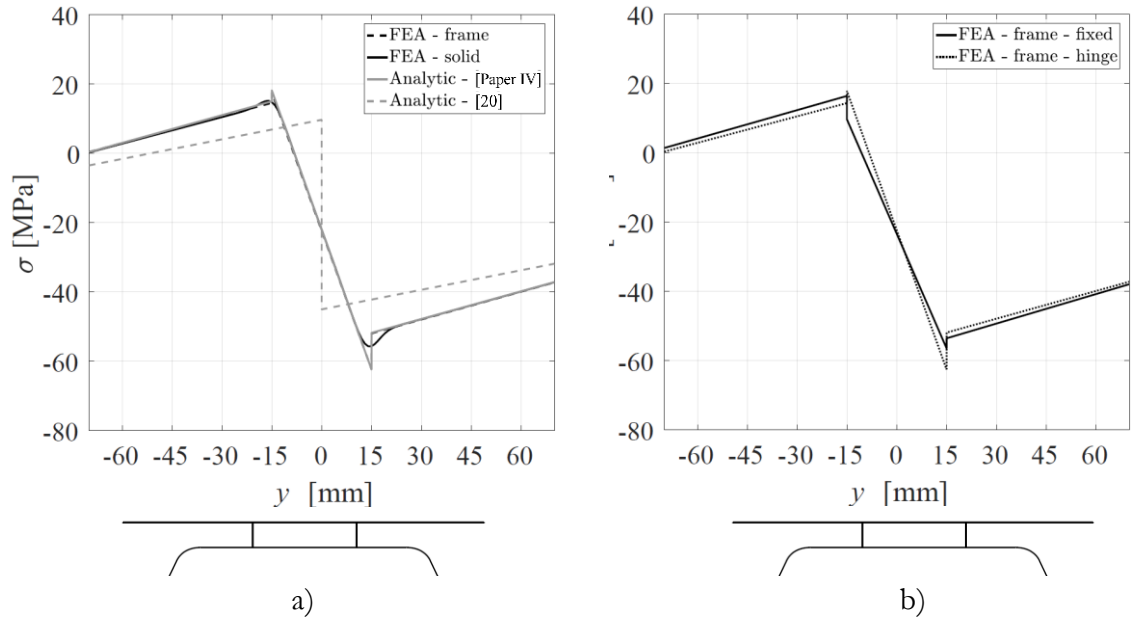

Figure 34. Normal stress distribution in the top fiber of the top face; a) comparison between 2D solid and frame numerical models and 1D analytical models and b) 2D numerical model with rotationally fixed core-to-face plate interaction at the welds compared to equivalent model with rotational hinge.

4.7.2 EXPERIMENTAL STUDIES

In order to verify the developed numerical and analytical analyses, experiments are conducted. The test setup is identical to that of the above presented case study and it is shown in Figure 35a. The experiment is repeated for two identical beams of conventional structural steel S355, here denoted as Beam 1 and Beam 2. For the output region (see Figure 33) the positions and names of the strain gauges in Beam 1 are shown in Figure 35b. The ten

strain gauges 4-13 are mounted in a single multi-channel gauge with an intermediate spacing of 2 mm between the gauges. The multi-channel device is located directly above the right weld line. For Beam 2, strain gauges corresponding to position 2, 3 and 14 in are installed.

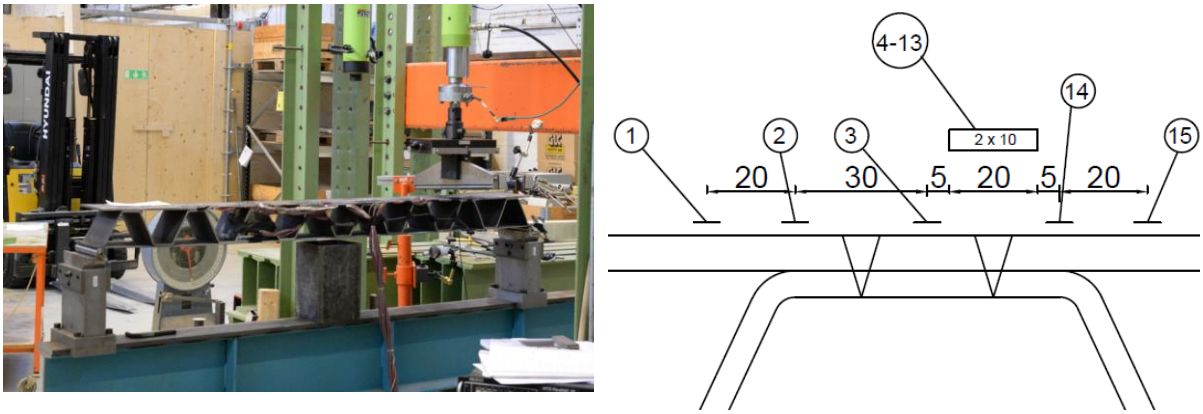

a) b)

Figure 35. Experiments; a) test setup, b) strain gauges at output joint.

The strain measurements from gauge 15 (Figure 35b) are shown in Figure 36a as a function of applied load. Figure 36a shows that the strain is close to linear, however with a modest curvature. The origin of this non-linearity is not assessed in detail, but can be related to both measurements and structural aspects. In order to display this non-linearity, a curve-fit of each strain signal is executed. The analytical expression related to the strain signal is then differentiated. The derivative of the strain signal is used to calculate a final stress for a 30kN applied load. Figure 36b shows the final normal stress from an applied load of 30kN, calculated by a linear load-stress-strain relation and using the derivative of the strain distribution of gauge 15. Thus, each strain signal yields an upper and a lower bound for the stress prediction (~42 and 46 MPa for gauge 15).

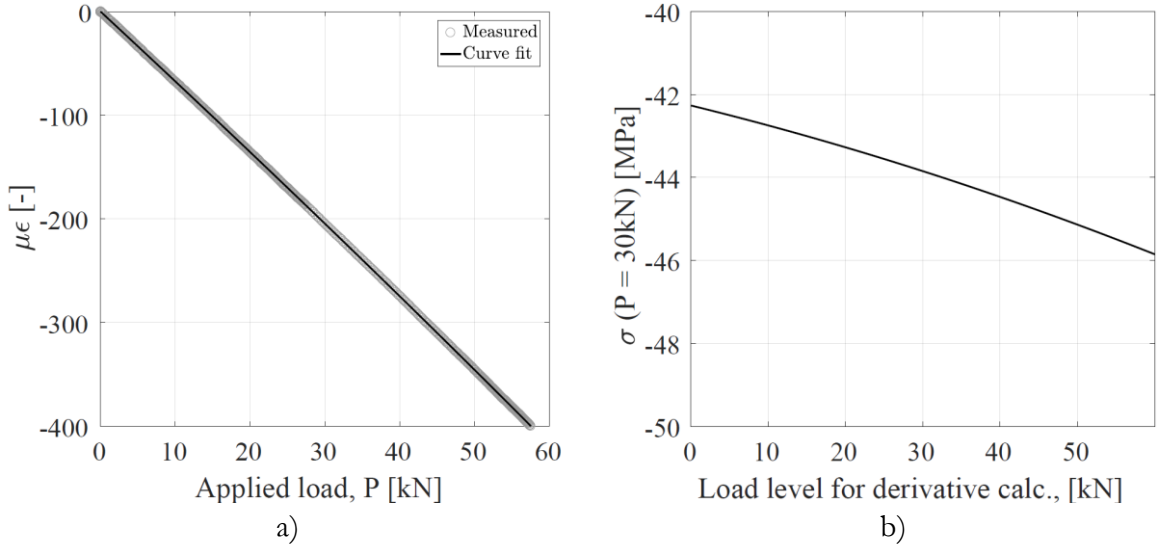

a) b)

Figure 36. a) Measured micro-strain as a function of applied load and curve-fitted function, b) final stress at a load level of 30kN as a function of the load-level for the derivative calculation.

Figure 37 shows the stress distribution on the surface of the top face as obtained from numerical analysis and measurements at a load level of 30kN. For the experimental results, the upper and lower bound stresses are indicated for Beam 1. The circular points in Figure 37 indicates the stresses when the derivative of the strains at a load level of 10kN is used. Apart from gauges 4-13, which belong to the multi-channel device, good agreement between the experiments and the numerical analysis is shown with a maximum deviation of ~4MPa (<10%). Gauges 4-13 show a difference in stress distribution compared to the numerical analysis. A clear explanation for the difference in measured and calculated strains in this local area has not been found and further, more detailed, analysis is needed to have a better insight into this problem.

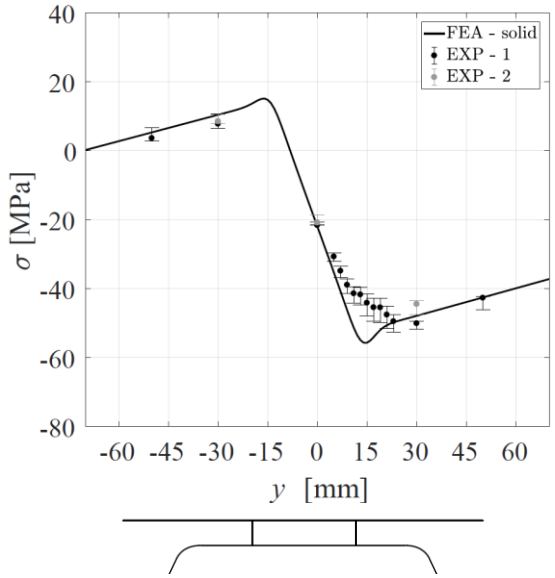

Figure 37. Stress distribution for the case study beam by numerical analysis and experiments.

In addition to the load-case that is described here in Section 4.7, another load-case is also tested. Both load-cases are shown in Figure 38. These tests are performed to failure and the result shows that the failure mechanism is a pure local plastic failure in the plates. Furthermore, no failure of the welds is identified either by visual inspection or by inspection of the test results. In the work that is presented in this thesis, a detailed study of these failure-tests is not included. That work is left for future studies.

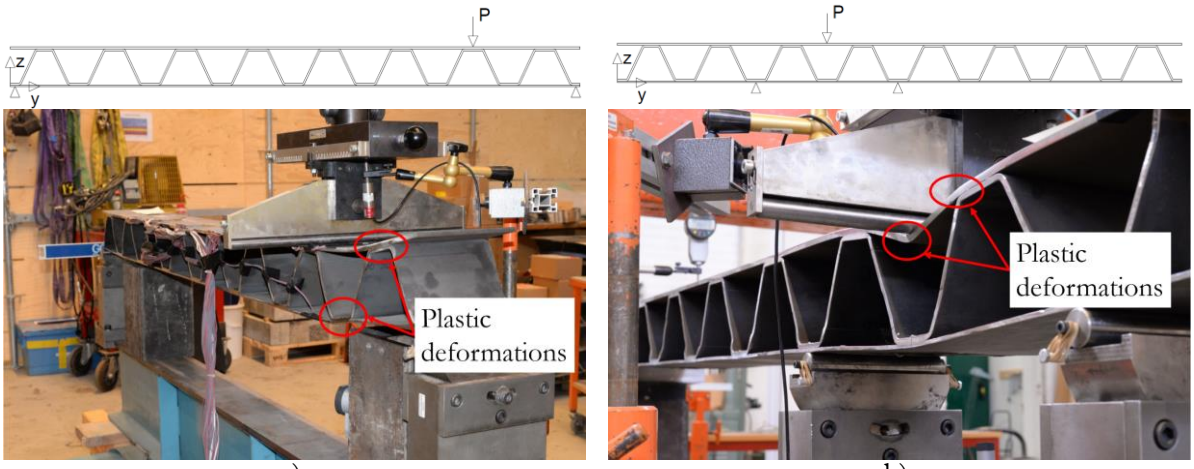

a) b)

Figure 38. Failure load tests; a) failure at support where panel-level shear force drives the deformation b) failure of loaded plate.

Thus, the experimental results verify the developed numerical analysis and the ESL approach for beam strips, which were described in sub-section 4.7.1. Furthermore, these analyses also verify the derived analytical solution for the transverse shear stiffness that is presented in Paper IV and utilised here. Also, the failure-tests indicate that the strength of the dual weld-line core-to-face joint is high. In fact, the results show that, both with respect to load-cases that concern pure panel-level shear and locally applied load, full plastic failure is developed without any failure in the welds of the joint.

4.8 FULL STRUCTURE

In this chapter the two investigated modelling approaches (which were described in Section 4.2) will be discussed from a full structure perspective, where the CCSSP deck is connected to a supporting system of longitudinal and transverse girders. This implies that the panel is not only subjected to out-of-plane loads, but also to in-plane loads due to the interaction with the supporting structure, see Figure 39. There exist two levels of accuracy that is of interest. The highest demand on accuracy is placed on approaches that are intended to be used in detailed design situations. Another level of accuracy that is of interest is for preliminary design situations, where lower demands are set. In the analyses that are shown in this section, core-to-face interaction is neglected, see Section 4.6. Here, a number of models, concerning a CCSSP deck together with the supporting girders, are used in order to investigate the two main modelling approaches. For more details on the models, see Paper III. A good structural analysis approach shall, independently of the sought level of accuracy, have the ability to:

- predict average deformations,
- predict stresses in all the constituent plates of the cross section and
- predict the stresses in the welds.

Five regions are selected for the comparative analyses that are performed in order to investigate the two structural analysis approaches (see Figure 40):

- Region subjected to panel-level sectional forces alone (Region *i*)
- Region subjected to panel-level sectional forces together with DAL (Region *ii*)
- Region subjected to panel-level sectional forces together with DAL in the vicinity of:
    - the main girder (Region *iii*-A)
    - the intersection of the main and the transverse girder (Region *iii*-B)
    - the transverse girder (Region *iii*-C)

In Figure 40 a single patch-load is shown for illustrative purpose. For the comparative analyses, individual load-situations are used for each investigated region, see Paper III.

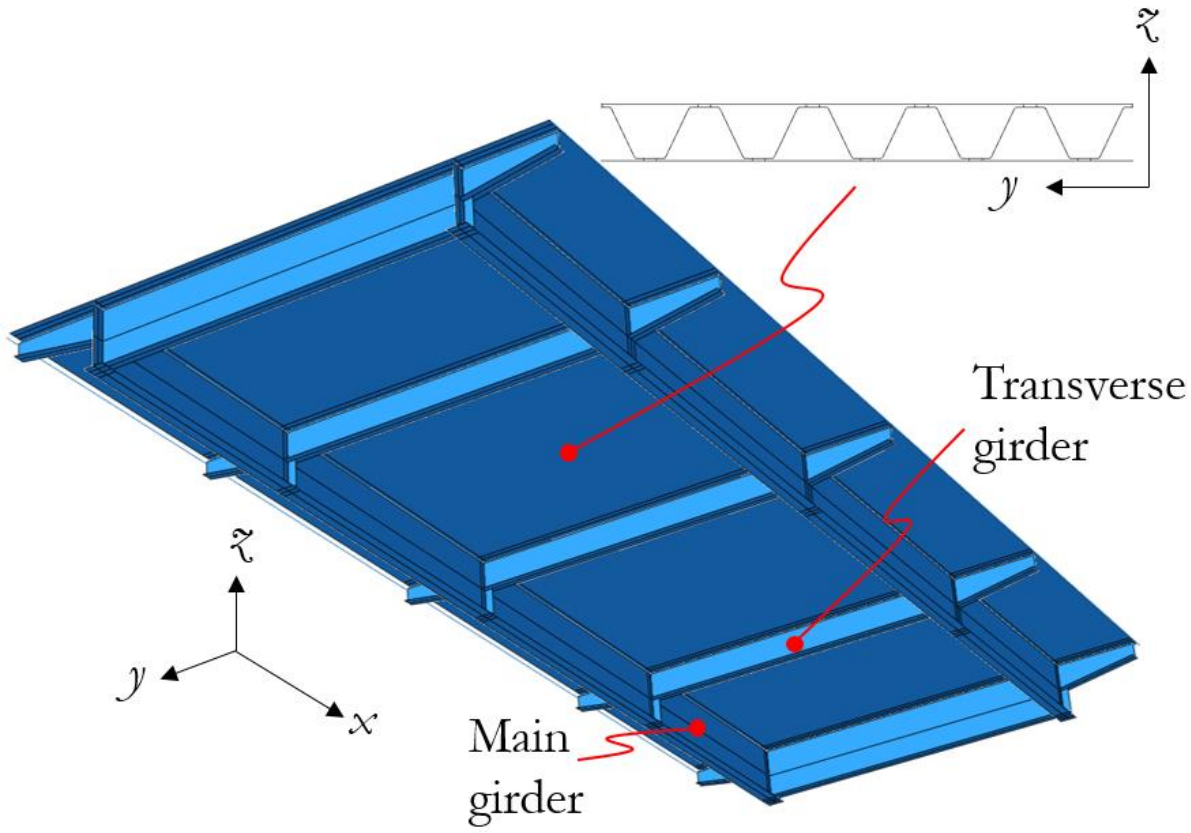

Figure 39. CCSSP in interaction with a supporting structure of longitudinal and transversal girders forming a full structure.

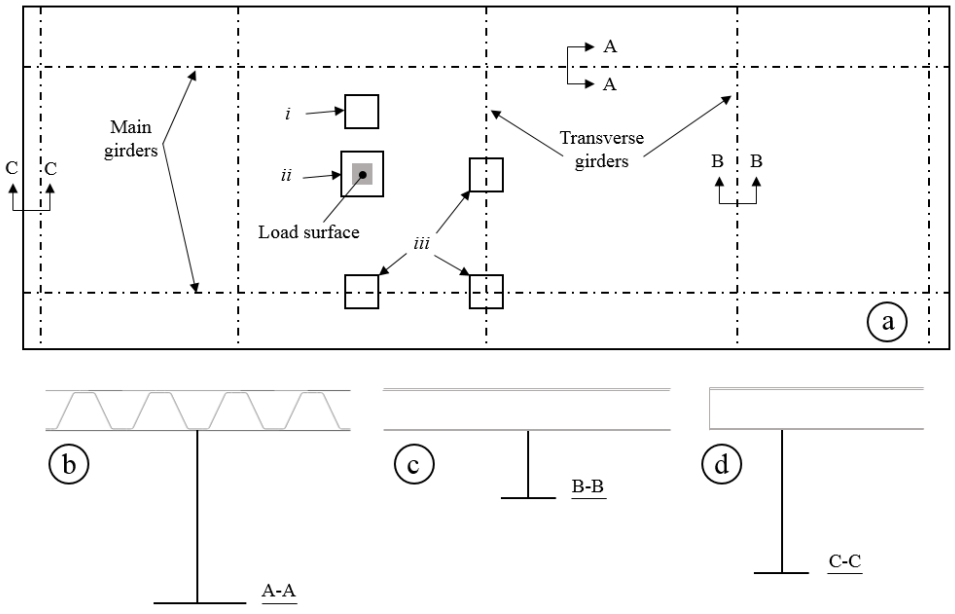

Figure 40. Investigated regions; *i*) area subjected to panel-level sectional forces alone, *ii*) loaded region and *iii*) at connection to supporting structure. a) View from above, b) section at main girder, c) section at intermediate cross-beam and d) section at end cross-beam [Paper III].

4.8.1 NUMERICAL MODELS

In order to apply and validate the sub-modelling and the ESL-approach, a number of numerical models are needed. In this sub-section, the principal models are shown. The reader is referred to Paper III for specific details. For the sub-modelling approach, a three-level multiscale model is adopted, see Figure 41. First a global model of the whole structure that incorporates an ESL deck is used (3D-1). Secondly, a first level sub-model that incorporates 3D-shell elements is used (3D-2). This model consists the full width of the bridge and a full span between the transverse girders, and 2 m additionally into the neighbouring span, see Figure 41. In all 3D shell element models that are utilised for the analyses that are described in in sub-section 4.8, the weld region rotational rigidity is incorporated according to Section 4.5. As the third level in the multi-scale model, a smaller shell element model is utilised (3D-3a) that has a more dense mesh compared to the larger model 3D-2. In order to verify the shell element model, an analogous solid element model is used (3D-3b).

For the ESL approach, the global model (3D-1) that adopts an ESL deck, is also utilised. However, as the output from the ESL analysis is limited to average deformations and panel-level sectional forces, the stress prediction needs further treatment, see Figure 24. For that reason, stress predictions are used based on the definitions of the cross-sectional constants, and an additional decoupled analysis for the effect of DAL is used, see Figure 42.

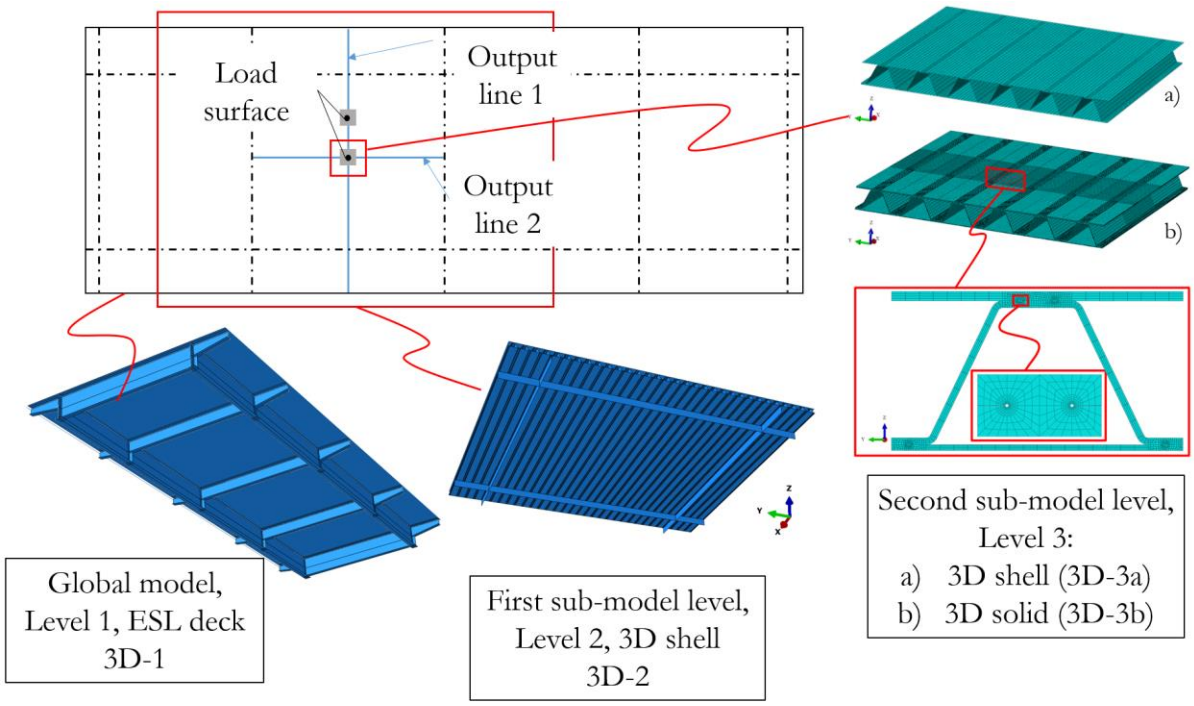

Figure 41. Three-level multiscale model for the ESL approach, and solid model 3D-3b for verification.

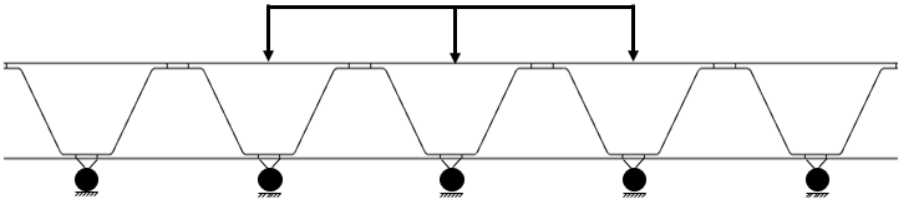

Figure 42. DAL-model for ESL-approach [Paper III].

One aspect that is important for the sub-modelling approach is the size of the first sub-model (i.e. 3D-2 in this case study). The deformations from the ESL deck of the global model, drives the nodes at the edges of the 3D shell element sub-model. The information that is contained in the ESL model only reflects the average deformation of the panel. Thus, the ESL model is incapable of predicting the natural deformations of CCSSP, see Figure 43. This imposes a modelling constraint for the three-level multiscale model that is adopted in the ESL approach for the full structure; the first level of sub-modelling (model 3D-2) needs to be large enough so that the interface between the 3D shell element model and the ESL model is placed sufficiently far from the studied location.

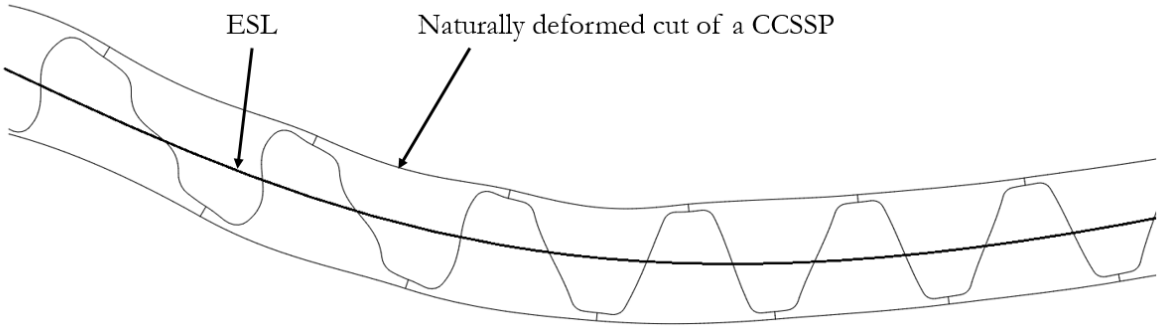

Figure 43. ESL deformations and natural deformation of a CCSSP.

4.8.2 DEFORMATIONS

Considering the prediction of deflections for the global model with an ESL deck (3D-1), it is validated in Paper III by comparison to the large 3D shell element sub-model (3D-2). The results considering vertical deflections are shown in Figure 40 and they originate from Output line 1 (see Figure 41) for 4 different loading cases, see Paper III. Here the deformation of the ESL-model is compared to the bottom face deformation of the 3D shell element model. This shows that the ESL-model can predict the average deformations with high accuracy for the investigated case.

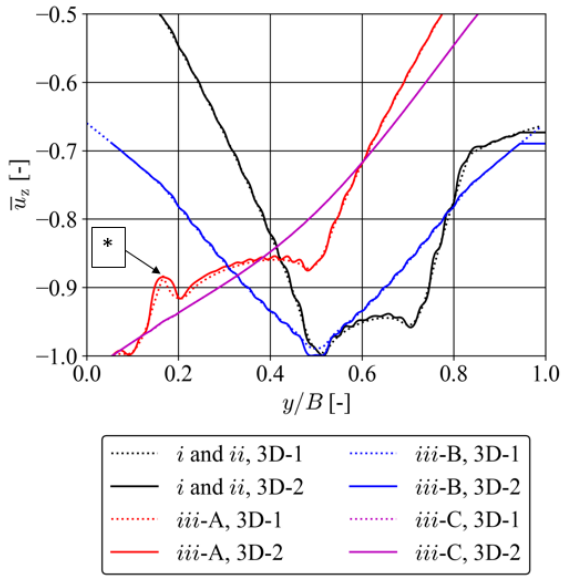

Figure 44. Vertical deflection of equivalent single layer model (3D-1) and 3D shell element model (3D-2) [Paper III].

4.8.3 PANEL-LEVEL SECTIONAL FORCES

In this sub-section, the capability of the ESL-model (3D-1) to predict panel-level sectional forces is investigated. The investigations are performed comparing the ESL-model (3D-1) and the 3D shell element model 3D-2, see Figure 41. In order to determine the sectional forces on the panel-level in the 3D shell element model, an integration of stress methodology is adopted, see Paper III. The orientations of the panel-level sectional forces are given in Figure 45.

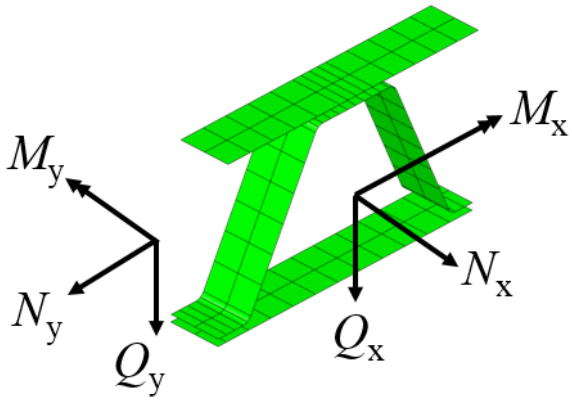

Figure 45. Orientations for panel-level sectional force, [Paper III].

The results from this investigation show that all investigated panel-level sectional forces (global effects) from the ESL-model 3D-1 are in good agreement with the results obtained from 3D shell element model with the exception of the membrane force in the weak direction, N_y. Figure 46 shows the distribution of N_y for the load-case and the two Output-

lines given in Figure 41. Inspecting the results from Output line 1 (Figure 46a), it is evident that the results are divergent, not only at the patch-loads location but also with a spread in the *y*-direction from the patch-loads. By investigation of the Output-line 2 in the *x*-direction (Figure 46b), the discrepancy has a constant magnitude in the regions from the transverse girder, up until the patch-load, where the error increases.

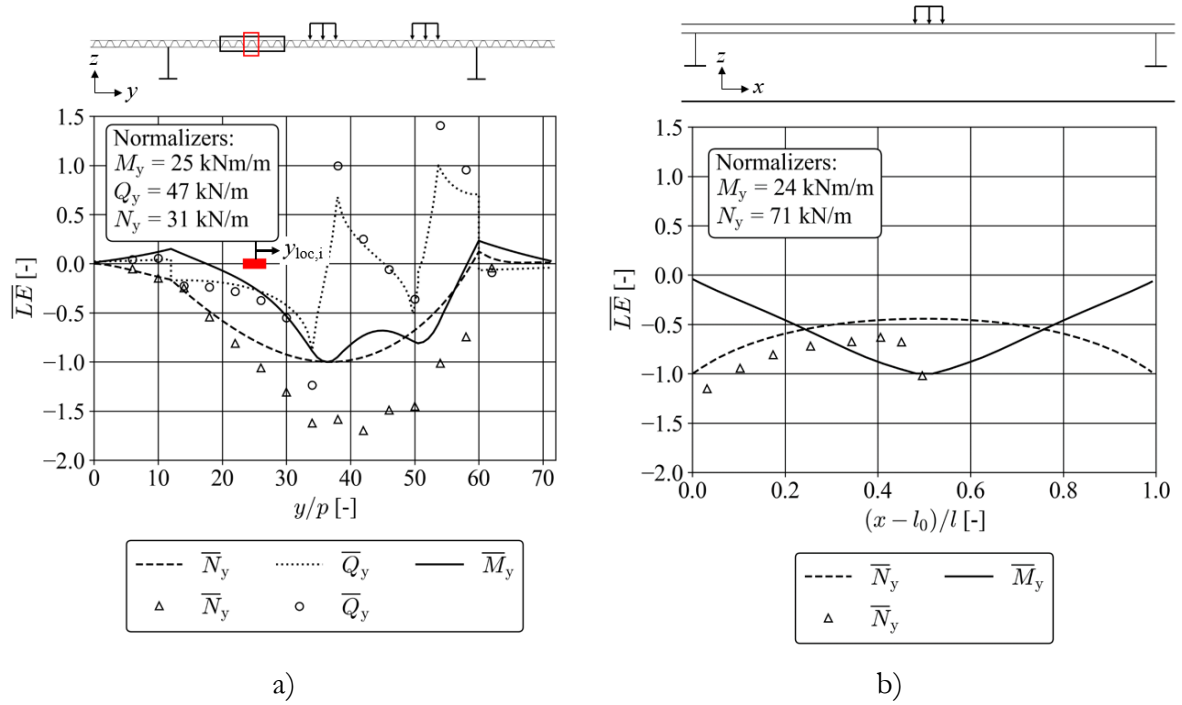

a) b)

Figure 46. Panel-level membrane force in the weak direction of the panel, N_y; a) Output line 1 and b) Output line 2, [Paper III].

Two possible sources for the discrepancy between the two models have been identified; the effect of through thickness compression and the panels shape-orthotropic property. Figure 47 shows principle figures of these two sources of error. When the CCSSP is subjected to a concentrated patch-load, or for locations at concentrated supports, a compression through the thickness of the panel occurs. Such local deformation can not be captured by the ESL model.

In order to validate the error from through thickness compression, a 3D shell element model corresponding to the loaded area of the panel is investigated, see Figure 48. In this analysis the vertical deflections are restrained, see principal sketch for a 2D section in Figure 42. The horizontal deformations are restrained at the position of the main and transverse girders. Figure 48 shows the distribution of membrane force in the *y*-direction for the top face, n_{Ny}. This is only one of the three constituent plates of the cross section, however, superimposing the membrane forces in all three plates shows that there exists an internal membrane force in the panel. The error from the through thickness compression is spread in the *y*-direction but cancels fast in the *x*-direction, see Figure 48. This explains the distribution of the error shown in Figure 46a and b.

A second source of error is the panels shape-orthotropic property, i.e. the neutral layer is different depending on what direction is considered, see Figure 47b. In the models that are

developed in Paper III, the ESL is modelled at the position of the stiff direction neutral layer. This yields an error for the forces in the *y*-direction. This error can be seen in Figure 46b for values of *x* on the left side of the load. For theses analyses a null-valued B-matrix is used, thus; there is no connection between membrane force and bending moment. Considering the *y*-direction, the null-valued B-matrix is an approximation. This effect has previously been described by e.g. Blaauvendraad [92] and in this case the source of error is confirmed by analysis of a corresponding symmetric deck panel. Here, the null-matrix has been assumed due to the small difference in *x* and *y*-direction neutral layer, and this effect is left for further investigations.

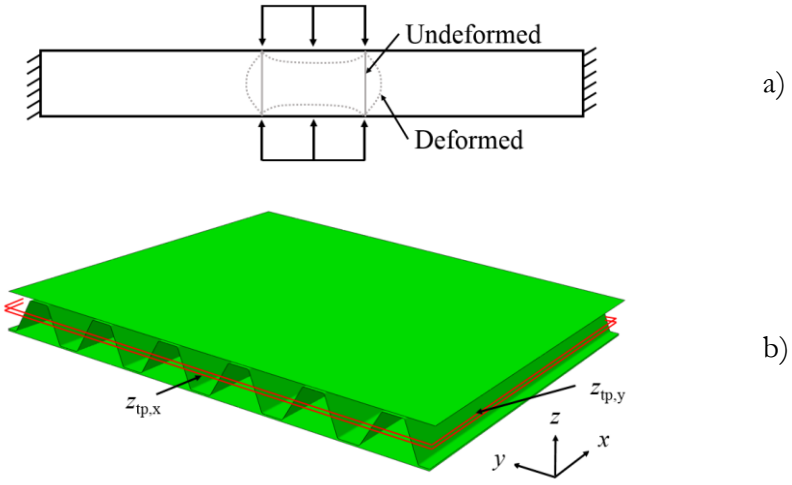

Figure 47. Sources of error in Equivalent Single Layer model for predictions of panel-level sectional forces; a) through thickness compression effect and b) effect of shape-orthotropy.

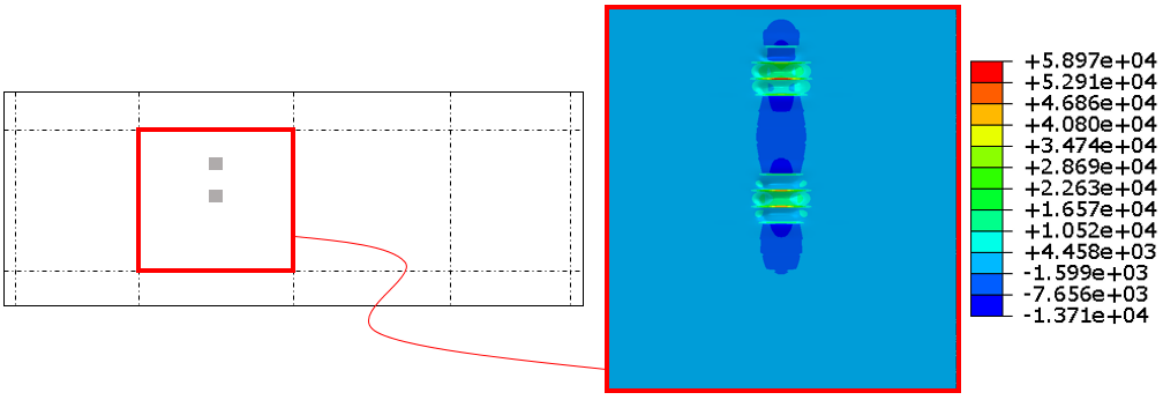

Figure 48. Membrane force, N_y-distribution in top face from 3D shell element model loaded by patch-loads and with restrained vertical deformations.

Another general error for ESL models is the boundary conditions. For the full structure that is considered here, this regards the interaction between the panel and the webs of the supporting structure. In the ESL, the rotations around the vertical axis of the deck are either coupled with the rotations of the main and transverse girders or free to rotate, i.e. hard or soft BCs, see e.g. Zenkert [33]. However, in the 3D case, the bottom face is attached to the supporting structure, causing an intermediately coupled connection. Thus, this is an inherent discrepancy between the 3D shell element model and the ESL model. Furthermore, the ESL

assumes FSDT, which also is an approximation to some extent that has not been investigated in detail in this thesis.

4.8.4 PLATE STRESSES

In the previous section, an error related to the membrane force N_y was discussed. This is described in more details in Paper III. However, the main aim of the design methodology is to predict stresses in the panel and the effect of this error on the magnitude of stresses in various parts of the panel depends on the contribution of N_y to the stresses in the constituent plates. Figure 49 and Figure 50 show the top and bottom face outer surface stress in the *y*-direction calculated from the ESL approach. These stresses are compared to those obtained from the 3D shell element model 3D-3a of the sub-model approach. Figure 49 show the stresses that are obtained from a location where panel-level sectional forces are acting alone, while Figure 50 shows a position that is subjected to DAL as well. It is evident that the stress predictions are not accurate enough for detailed design calculations. Figure 49 and Figure 50 show that the impact of the membrane force N_y is modest, which leads to the conclusion that the error in stress values is related to other sources. One error that is related to the panel level sectional forces concerns a constraint effect that origins from the stiff direction bending action and cause a membrane action in the faces in the weak *y*-direction, see Paper III.

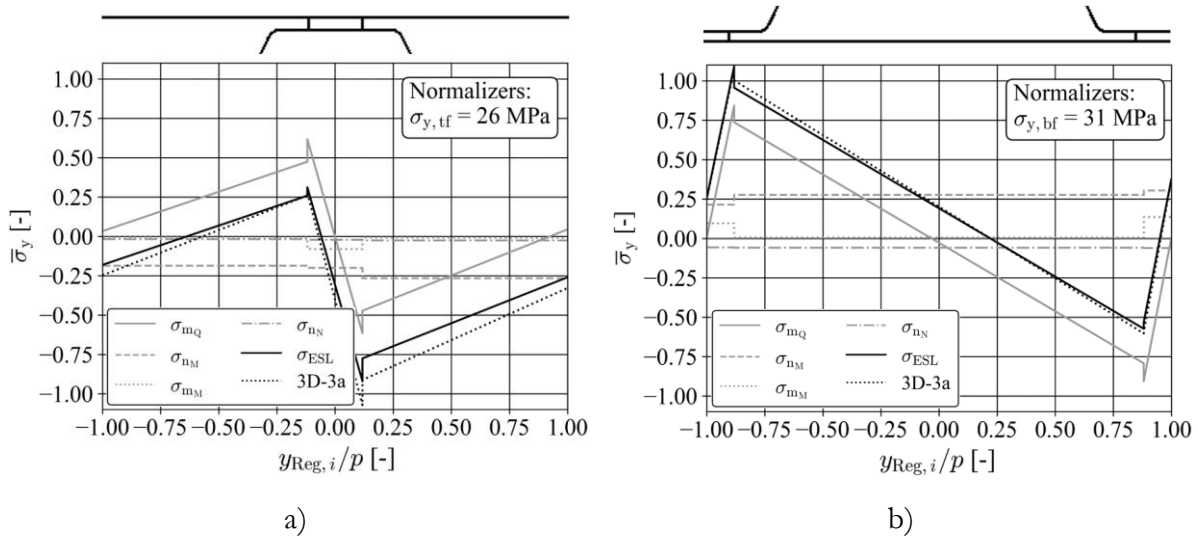

a) b)

Figure 49. Comparison of stresses for the ESL-approach and a 3D shell element (3D-3a) model in a region subjected to panel-level sectional forces alone; a) top face, and b) bottom face [Paper III].

Figure 50a shows that the top face stresses are well predicted using the ESL approach for the region directly under the DAL. However, the bottom face stresses are predicted with a low accuracy. Here the results are shown for a DAL model according to Figure 42. However, different DAL models have been investigated (spring supports and incompressibility conditions, see Paper III) and the results show that they do not lead to more accurate predictions. As the error is pronounced in the bottom face, the miss-prediction could originate from the spread of forces in the *x*-direction, that is overseen in the 2D DAL model that is utilised here. However, analogue 3D-analysis show only a moderate difference when compared to the 2D DAL model. This leads to the conclusion that the system is highly coupled and that the global and local systems can not easily be decoupled in this way when an accuracy that can be used for design purpose is sought. Here, only the face plate stresses are investigated. However, investigating these stress distributions in the regions of the welds, one can conclude that the weld stresses are not in agreement for the two modelling approaches. These conclusions are drawn with respect to regions at local loads. It is not expected that the modelling approach will be accurate in the regions that include connecting points to the supporting structure, which are more complex in their nature.

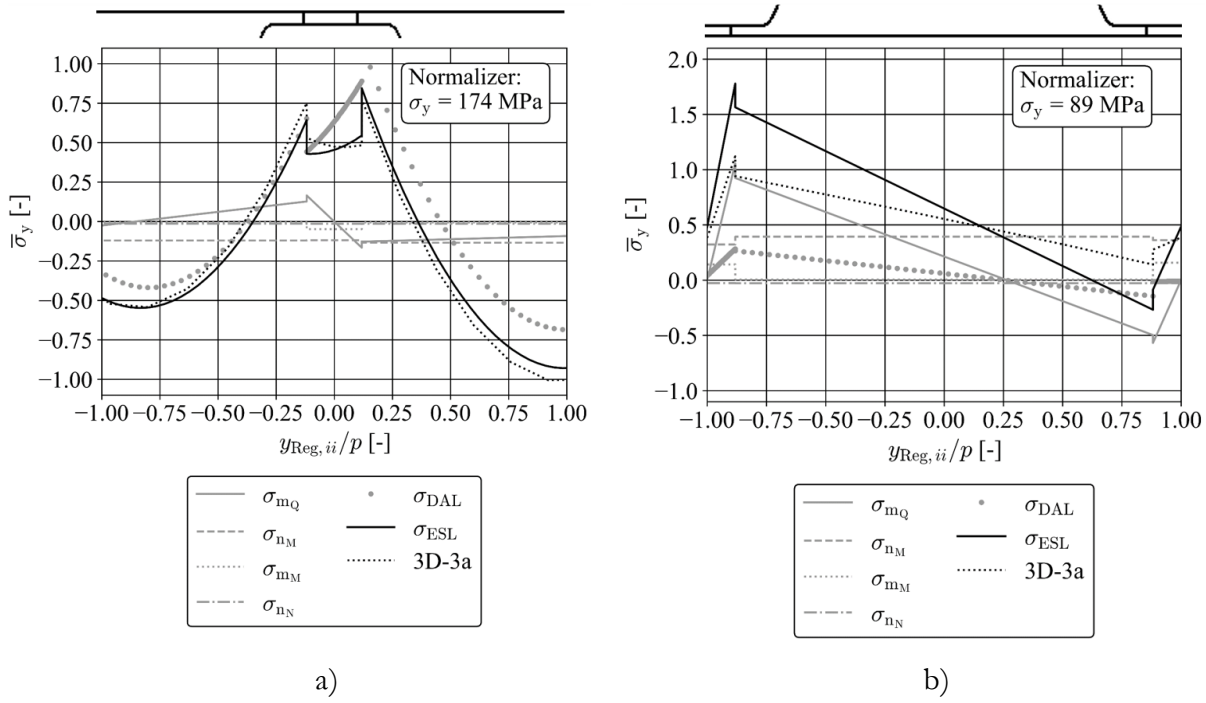

a) b)

Figure 50. Comparison of stresses for the ESL-approach and a 3D shell element model (3D-3a) in a region subjected to panel-level sectional forces and directly applied load (DAL); a) top face, and b) bottom face [Paper III].

The ESL-approach can not predict stresses in the constituent plates of the cross-section with high accuracy. In the previous paragraphs, the 3D shell element model (3D-3a) was used as a reference to investigate the capability of the ESL-approach. In Figure 51, the results from 3D-3a are compared to the solid element model (3D-3b) regarding normal stress in the y-direction, σ_y at the outer surface of the top and bottom faces and the core. This again relates to region *ii* that is subjected to panel-level sectional forces and DAL. The results shown in Figure 51 validates the general concept of using 3D shell elements for the design of CCSSPs as well as the sub-modelling approach, for stress prediction of the constituent plates. However, this is under the conditions that the weld region rigidity is incorporated according to sub-section 4.5. In paper III it is also shown that the regions in the vicinity of the supporting structure can be modelled with high accuracy using this approach. In addition, these regions are shown to be sensitive to the modelling of the connection between the bottom face and the web of the supporting structure.

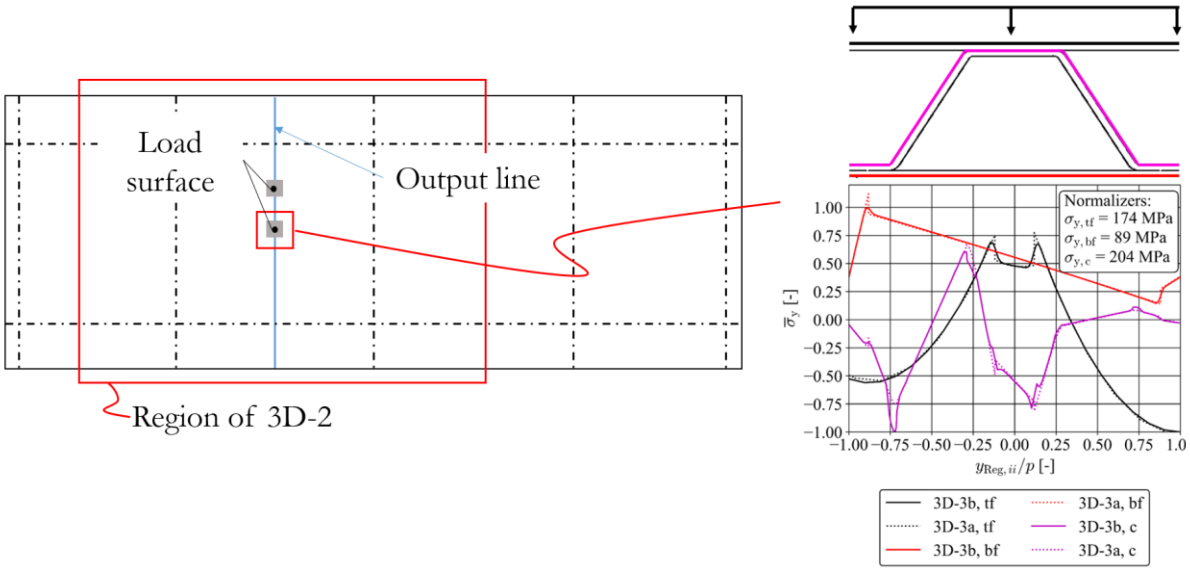

Figure 51. Position and load situation for Region *ii* and normal stress in the outer surface of the top and bottom face and the core for shell and solid models 3D-3a and 3D-3b, respectively [Paper III].

4.8.5 WELD STRESSES

As the ESL-approach is not able to predict the stresses in the constituent members with a high accuracy, this approach is not used to evaluate the stresses in the welds. Instead, the sub-modelling approach is used for this purpose. The results show that the sub-modelling approach can predict stresses, also in the welds, with a high accuracy, in all the five regions shown in Figure 40. Thus, the results show that a 3D shell element model can be adopted for prediction of the nominal stresses in the welds. For this investigation a solid element model is used as a reference. Figure 52 shows a comparison between the solid and shell element models regarding the nominal stresses in the weld, again for Region *i* (see Figure 51). Again, for these analyses the weld region needs to be modelled according to Section 4.5 where a rotational spring element with a stiffness according to Paper V is incorporated, in order to reach sufficiently high accuracy. The stresses that are calculated according to the sub-model

approach that is validated in Paper III, can be used in conjunction with the nominal stress fatigue strength that is derived in Paper II in order to estimate the fatigue life of the deck. Another aspect that is of high importance is the modelling of the connection between the main girder web and the CCSSP deck. In this region, the laser welds are in the direct vicinity of the welds that joins the bottom face to the deck. Here the distribution of the weld thoughts that connects the deck to the main girder webs needs to be incorporated in order to obtain proper weld stress predictions in the bottom core-to-face joint, see Paper III.

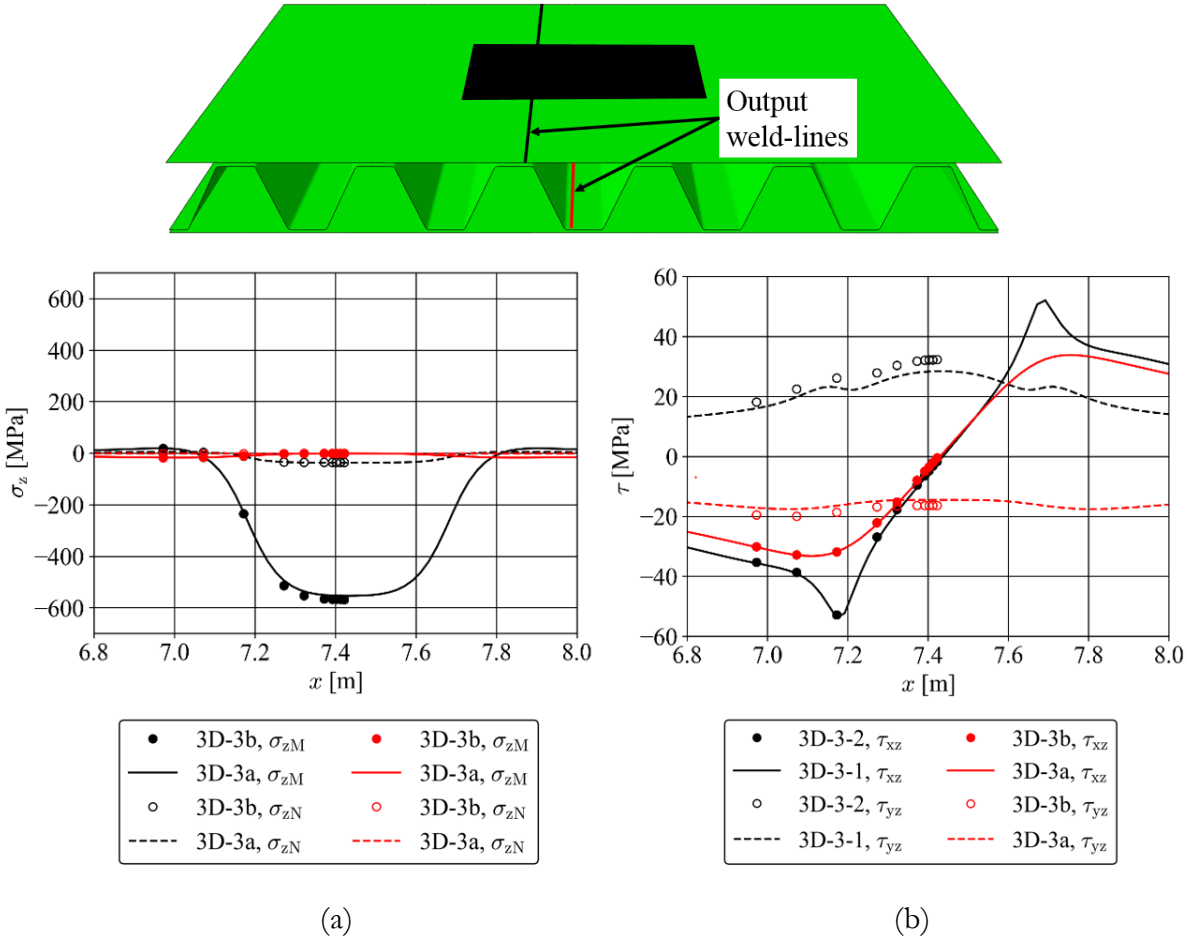

Figure 52. Comparison between shell element model 3D-3a and solid element model 3D-3b with respect to weld stresses; a) normal stress from axial force and bending, and b) shear stress parallel and perpendicular to the weld line [Paper III].

4.9 DESIGN ASPECTS

The work presented in Paper III and discussed in the previous sections aimed at the establishment of a structural analysis method that can be used for design purpose. However, outside the scope of Paper III, several design aspects of the all-steel bridge concept are also considered. Here, the aim is not to do a full structural design of a bridge, but rather to point out several important aspects that need to be considered in bridges with a CCSSP deck.

With respect to Serviceability Limit State (SLS), the design calculations are a straight forward task to solve. The structural analysis can be performed with an ESL model of the deck and compared directly against the requirements given in design codes. In the Eurocodes the global deflection is restricted to $L/400$ (CEN [93]) where L is the length of the main girder, the cantilever, or the minimum panel width for the deck sections that are limited by the main and transverse girders, see Figure 53.

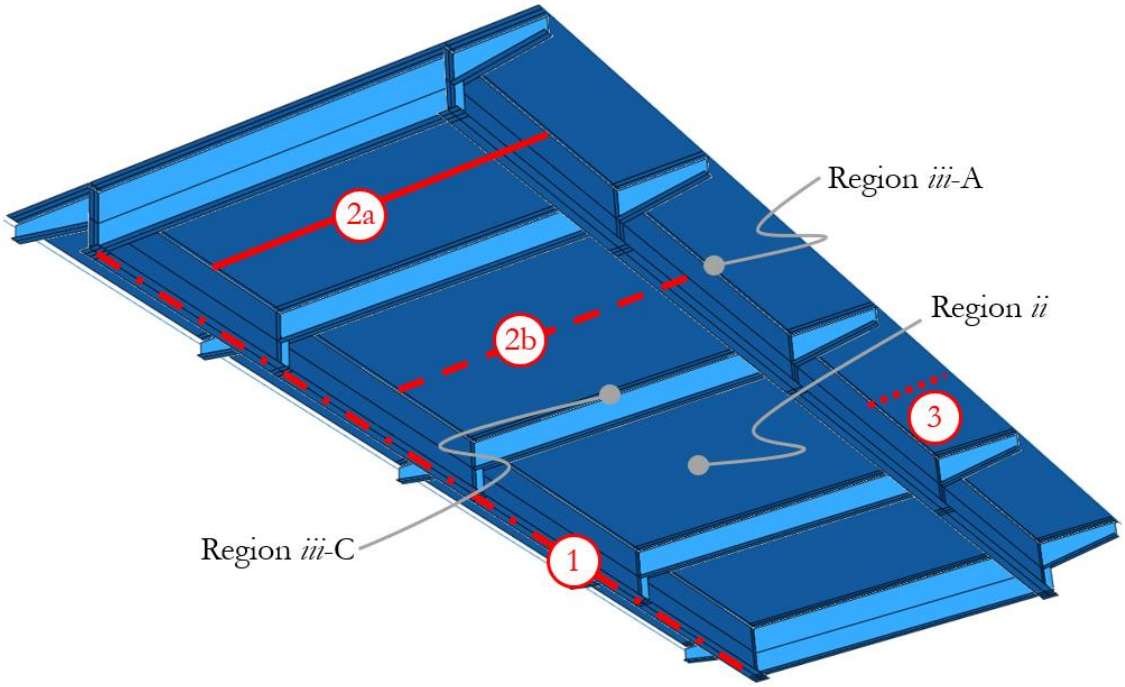

Figure 53. Parts of the bridge that are controlled for deformations; 1) main girder, 2) deck, and 3) cantilever.

Considering the Ultimate Limit State (ULS) design controls, three regions of the deck have been identified to be of specific interest here. These regions are Region *ii*, Region *iii*-A and C, with the same notations as in Paper III, see Figure 53. Region *ii* is in the center of the deck span at the position of the wheel pressure, see Figure 54. Here, the main aspect in design, for the plate elements, is the top face plate. It is subjected to compression membrane action in the *y*-direction, n_y from the panel-level bending moment in the *y*-direction, M_y. Another action that also yield a significant contribution to the full state of stress is the stiff direction panel-level bending moment, M_x that gives rise to membrane force in the *x*-direction, n_x. Thus; a plate field under the wheel pressure is subjected to bi-axial compression. In addition to the bi-axial compression, local bending in the *y*-direction, m_y from DAL and panel-level shear-force, Q_y is present. In the general case there will also be an in-plane shear force n_{xy} present to some extent. In order to perform a buckling capacity control for this state of stress, with the Eurocodes as a basis (CEN [93]), there are two possible methodologies to adopt, either the reduced stress method (CEN [94], Zizza [95]) or a full non-linear analysis with respect to material and geometry. DNV [96] also give some guidance that can be used for approximate calculations. Here, as in all parts of the deck that are subjected to wheel pressure, there will also be a significant bending action occurring in the welds.

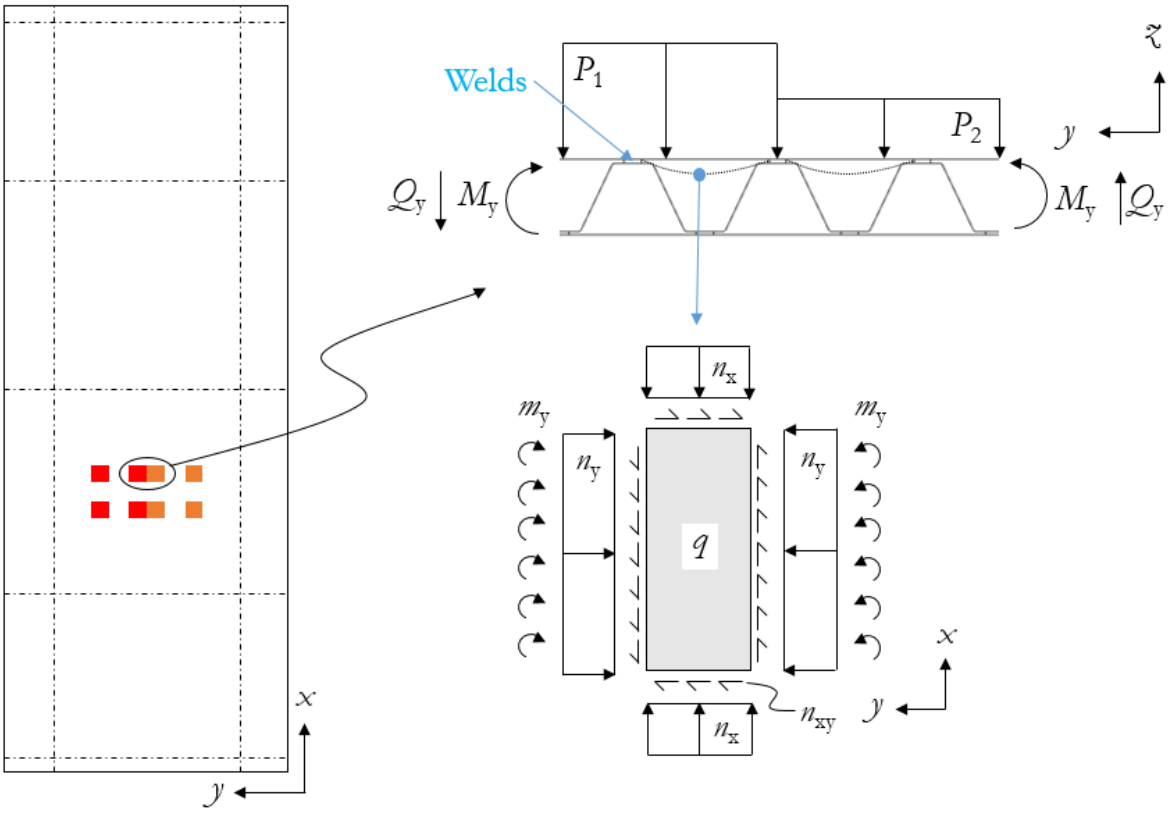

Figure 54. Load situation for Region *ii*.

At the positions close to the main girder, Region *iii*-A (see Figure 55), there is another complex state of stress occurring. Here, M_y instead cause tensile membrane action in the *y*-direction for the top face plate. However, for the bottom face (plate field 2 in Figure 55), the corresponding force (n_y) is compressive. The global action of the main girder cause panel-level membrane action in the stiff direction, N_x and thereby also in the bottom face plate, n_x. As the panel is acting as an upper flange for the main girder, there will also be a significant amount of in-plane shear stress present in this plate field. In addition, bending moment in the *y*-direction from Q_y is present.

Another plate field of specific interest is the corrugation leg that is in the vicinity of the main girder web (plate field (1) in Figure 55). Here, compressive membrane force from Q_y and from the patch-load interact.

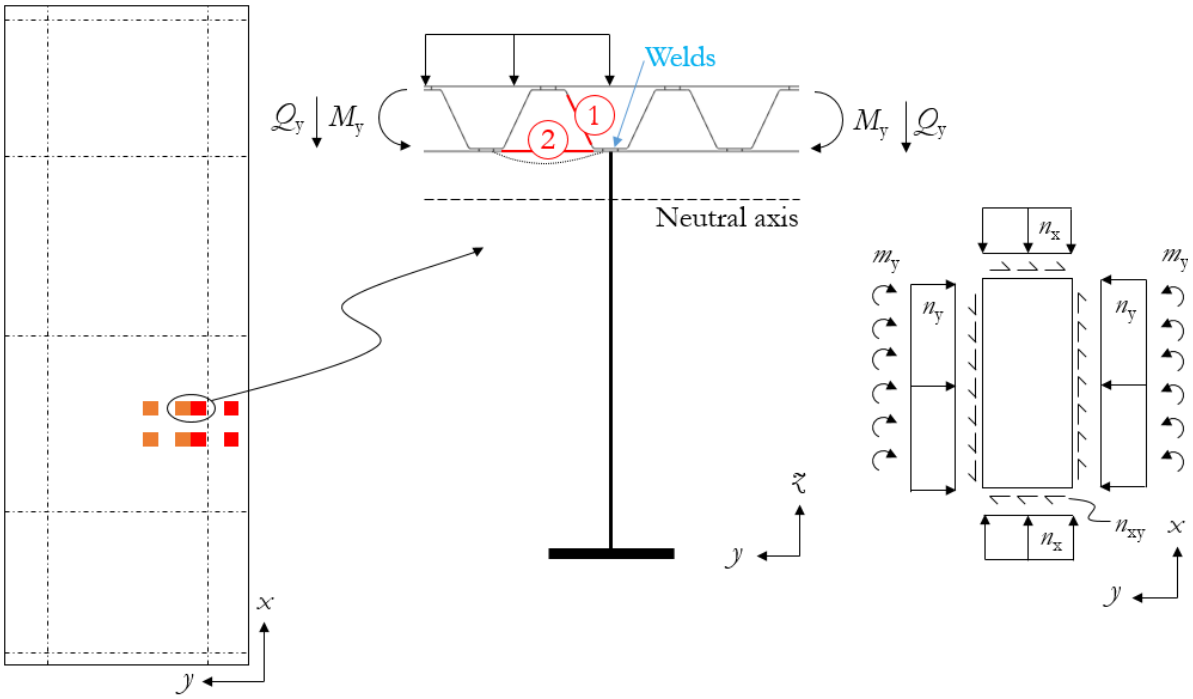

Figure 55. Load situation for Region *iii*-A.

In Region *iii*-C, the attention is directed towards the bottom face connection to the transverse girder, see Figure 56. Here, the results from Paper III show very high weld-stresses originating from both axial force and bending moment acting on the weld. The high axial force is a result of the load-transfer from the applied patch-load to the transverse girder, see Figure 56. This is both with respect to distribution considering the yz-plane where the load is transferred through the narrow weld (here assumed to be 2 mm) and the xz-plane where the load is transferred to the web of the transverse girder with a limited distribution width at the level of the bottom core-to-face weld. This concentration of the stress-flow through the thickness of the sandwich panel also has an effect on the core plate stresses at the bottom side at the transverse girder and in the transverse girder web under the stake-welds. Here, controls for concentrated loads have to be performed. Regarding the high bending moment in the welds, it is related to the fact that the transverse girder provides a line-support for the bottom face of the panels, see Figure 57. Thus, in a line, the bottom face is constrained and the core is free to deform. This leads to a rotational difference between the two plates and significant bending action in the weld.

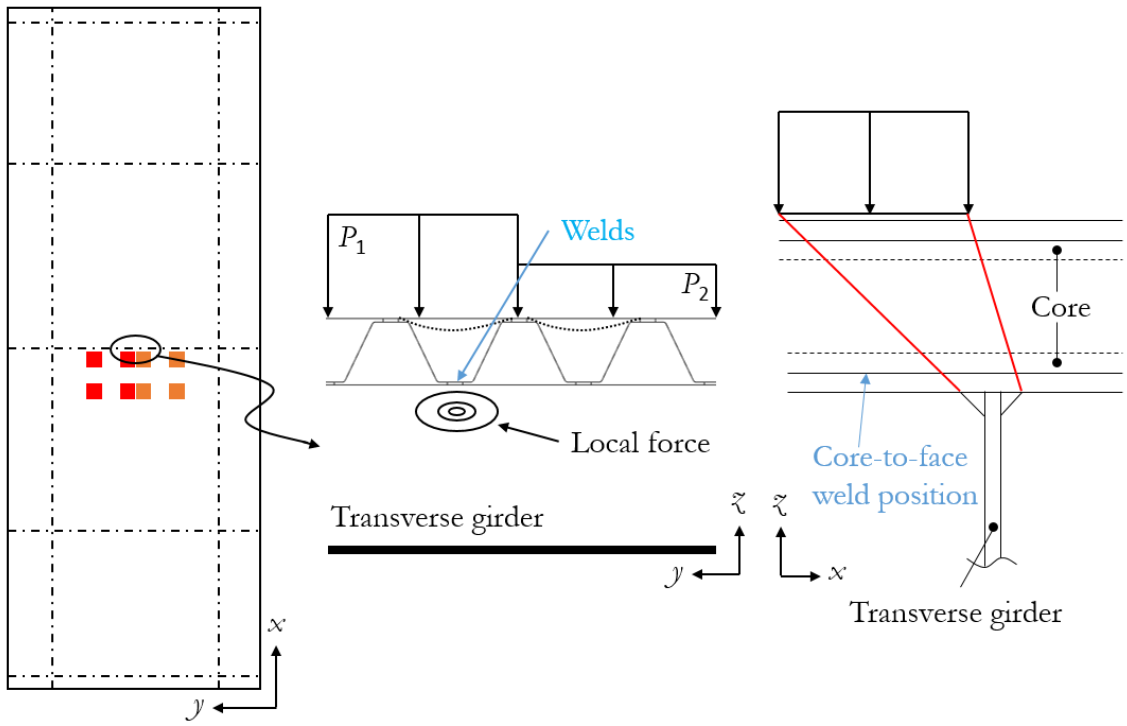

Figure 56. Load situation for Region *iii*-C.

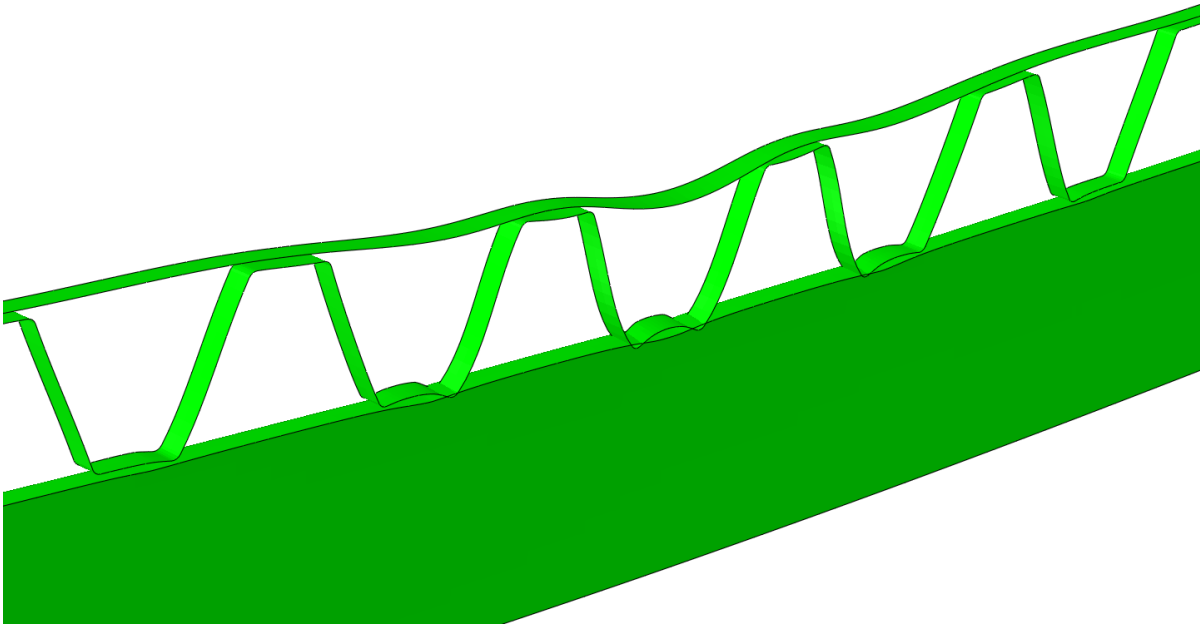

Figure 57. Deformed shape at transverse girder, scale factor = 50.

The analyses that are performed for this sub-section, with full traffic loads according to [93], show that the utilisation ratio for the plate fields is in some cases high. In fact, up to 2 for the plate fields in Region *ii* and *iii*-A. The capacity calculations are approximate and full non-linear analysis or the reduced stress method are not adopted. Furthermore, as is also shown in Paper III, high stresses in the top face welds under the patch-loads and the bottom face at the transverse girder are identified as critical. In both cases, bending action is the main contributing factor to the stress. A utilisation ratio for static design of approximately 7 is identified for the most critical welds in the bottom face. In order to decrease all the above-mentioned high utilisation ratios, topology optimisation concerning the full structure is needed in order to find material-efficient CCSSP decks. One factor that is limited by the welding process is the weld width. In Paper I, the weld widths were measured to around 2mm in average and that was adopted in the analyses. Increasing the weld width will decrease the stresses at the bottom core-to-face joint and also in the top core-to-face joint under the patch-load, see Paper I. For the highly utilised bottom core-to-face welds at the transverse girder, increasing the bottom face thickness will decrease the weld stress. Thus, one possible alternative solution is to increase the bottom face thickness locally, directly above the transverse girder. In fact, analyses show that increasing the bottom face thickness locally to 20 mm and increasing the weld width from 2 to 4 mm decreases the utilisation ratio in the bottom face welds from 7 to 2. This level of utilisation is possible to address with updating the other geometric properties of the CCSSP from the results of topology optimisation.

5 SUMMARY AND CONCLUSIONS

This thesis is concerned with the study of CCSSPs for bridge applications. Focus has been on three main topics: production, fatigue performance and methods for structural analysis. In the following, some general conclusions of the work are listed. More detailed summary of results and conclusions are given thereafter for each of the three focus areas of the work.

1. CCSSPs have good potential to replace conventional orthotropic plates as bridge decks. Possible savings in both material and production costs are demonstrated, providing an economically and environmentally more sustainable solution.
2. Laser welding is capable of producing good quality panels in a fast, and atomised production process.
3. The plates show good stiffness and strength properties. Furthermore, a ductile behaviour in Ultimate Limit State is demonstrated including the laser welds.
4. The fatigue performance is high. This is demonstrated for a large-scale panel subjected to wheel loads larger than the load given in current recommendations. No failure could be detected after the panel had been subjected to 8.2 million load cycles.
5. CCSSPs are complex elements with respect to structural behaviour. Detailed models are needed to capture local load effects, particularly with reference to fatigue.

PRODUCTION

- The welding-process used to produce laser-welded CCSSPs is capable of reaching the predefined quality targets in terms of weld dimensions and panel geometry.
- Few cases of less satisfactory geometric quality are identified, and their origin is discussed in this thesis. As an example, the weld cross-section geometry is hard to control if contact between the two plates that are to be joined is not achieved during welding.
- The adopted production methodology yield weld widths that varies between 1 and 4 mm and weld misalignments equal to or less than 2mm for 70% of the measured cases. A larger scatter is obtained for the gaps between the welded plates.
- Regarding the impact of the production-dependent geometric properties on the effective notch stress in the weld, both the weld width and the misalignment has a strong influence within their measured natural variation. In addition, the results show that an increase of the weld width, can lead to either an increase or a decrease of the fatigue-relevant weld stress.
- The plate gap has no or very modest effect on the effective notch stress, if contact interaction between the core and the face plates is excluded from the analysis.
- However, the plate gap has a significant effect on the effective notch stress, if contact interaction between the core and the face plates is included in the analysis. This originate from the strong effect of the gap height on the load-magnitude at which contact occur.

FATIGUE

- The results from the cell-specimen tests agree well with other test data obtained from fatigue-tests of web-core sandwich panels, independent of crack-mode, joint configuration, stress-range and loading condition. This indicates that there is no significant difference in fatigue strength of laser-welds in CCSSPs, compared to other core geometries.
- Based on the evaluation of the test data that is presented in this thesis together with existing data, recommendations for fatigue-design considering the effective notch stress as a fatigue parameter are made. The results show that the current recommendation that is given by IIW can be used, if loading in the high stress-range ($< 10^4$ cycles to failure) does not occur.
- Regarding the nominal stress approach, and failure-mode of cracking through the weld, a characteristic fatigue strength at 2 million cycles of 57 MPa is derived on the basis of a fixed slope coefficient of 3.
- A fatigue-failure mode that concerns cracking with an initiation at the root of the weld and propagation through the base plate, is identified. This failure-mode can occur in CCSSPs when a splitting action is present at the side of the fatigue-life determinant weld.
- The results obtained from the fatigue tests of the cell-specimens indicate that the nominal stress fatigue-strength is higher for the case of cracking through the base plate compared to cracking through the weld.
- The results obtained from the fatigue tests of the cell-specimens indicate that the fatigue-strength is higher for the Duplex stainless steel compared to the conventional structural steel.
- The fatigue test of the panel-specimen indicate that the fatigue-performance of CCSSPs is very high. The tested panel survived 8.2 million cycles, when subjected to a wheel load larger than that specified for fatigue design in Eurocode.

STRUCTURAL ANALYSIS

- The derived analytical solution for the weak direction transverse shear stiffness is accurate and the stiffness definition can be used to predict stresses in the constituent members of a CCSSP subjected to pure shear. This is validated by numerical analysis and experiments.
- Regarding the weak direction panel-level bending, the results indicate that, the dual weld-line configuration has no effect on the equivalent stiffness. However, this configuration yields a local bending action of the face plates between the welds, which does not occur in the single weld-line configuration. This has an effect on the state of stress in the welds.
- The results indicate that the core has a modest contribution to the equivalent membrane stiffness in the weak direction of CCSSPs.
- Regarding beams and for positions away from loads and BCs, the ESL approach show good agreement to numerical analysis with continuum elements. However, for a full

structure, the ESL approach give considerable miss-predictions for some cases, especially in the bottom face.

- Another indication that is obtained from the results is that the ESL models, which are the basis for both the ESL approach and the sub-modelling approach, can predict average deformation with a high accuracy. This implies that the ESL models can be used for design calculations in the Serviceability Limit State.
- The results indicate that the sub-modelling approach - comprising shell elements - has a high accuracy concerning prediction of stresses in all the constituent members of the cross-section, including the welds. This conclusion is based on verification by analyses consisting of solid elements. A condition for this is that the core-to-face joint is modelled such that it represents the stiffness of the joint properly. The presented modelling strategy including rigid connections and elastic springs fulfils this condition.
- Also, the results show that, regarding incorporation of the deformability of the weld region in the structural analysis, the rotational stiffness is the deformation that has the strongest influence on the weld stress.
- For 2D and 3D analyses, the derived closed form solution for the rotational stiffness of stake-welds connecting two parallel plates yields accurate results.
- Contact action between the core and the face plates has a strong influence on the state of stress in the welds. Also, the position of the contact is important for this stress.
- In general, the contact between the core and the face plates decrease the weld stresses. However, there exists cases were the contact action has reversed effect.

6 FUTURE WORK

The work conducted in this thesis, together with findings from previous studies, indicate that CCSSPs have very complex load-bearing behaviour. This makes the task of finding weight-efficient bridge decks hard. In this aspect, full structure topology optimisation is needed. Such optimisation can be based on the sub-modelling approach presented in this thesis. A condition for the implementation of the sub-model approach is that it is validated by several additional topologies in future work. Alternatively, future efforts can be devoted to development of more time-effective calculation approaches as the micro-polar plate theory or numerical models with "super-elements".

One aspect that has been shown to be of outermost importance is load effects in the welds. Increasing the weld width can reduce the weld stresses. To this end, optimisation of the welding procedure with the target of maximising the weld width is of interest for future studies. Another factor that lead to reduced weld stresses is contact between the core and the face plates. For this reason, the development of production processes that can ensure initial contact between the plates would be of high value for the continued development of this deck concept.

The intersection between the panel and girders that are oriented perpendicular to the core elongation was shown to be a region were the weld stresses are high. Future studies that has a focus on this region would thereby be of importance.

As was stated in section 1.4, the panel-to-panel joints were left outside of scope of this thesis. However, this is a highly relevant aspect of larger CCSSPs and development of such joint is of major importance. In this regard, both manufacturing and structural aspects needs to be considered.

Another topic that can be the target for future investigations is the use of structural filling of the core voids as it has shown great promise regarding further weight-reductions.

Fatigue is a topic were the strength of an investigated detail has a strong relation to the number of existing tests. In this regard there is a need of further testing, most importantly regarding panel-tests (where a higher degree of multi-axiality is incorporated), tests of Duplex stainless steels, and tests regarding crack-modes that initiate at the root of the laser-weld and propagates through the core.

7 REFERENCES

[1] PANTURA, [Online]. Available: https://www.chalmers.se/en/projects/Pages/Pantura.aspx. [Accessed: 17-Feb-2020].

[2] PANTURA, "D5.3 - Needs for maintenance and refurbishment of bridges in urban environments," 2011.

[3] P. Arrien, J. Bastien, and D. Beaulieu, "Rehabilitation of bridges using aluinum decks," *Can. J. Civ. Eng.*, vol. 28, no. 6, pp. 992–1002, 2001.

[4] V. Mara, R. Haghani, and P. Harryson, "Bridge decks of fibre reinforced polymer (FRP): A sustainable solution," *Constr. Build. Mater.*, vol. 50, pp. 190–199, Jan. 2014.

[5] Intelligent Engineering, [Online]. Available: https://www.spstechnology.com/our-sectors/bridges. [Accessed: 17-Feb-2020].

[6] D. K. Harris, "Component sizing approach for the sandwich plate system," *Struct. Infrastruct. Eng.*, pp. 1–13, Sep. 2010.

[7] M. H. Kolstein, "Fatigue classification of welded joints in orthotropic steel bridge decks," *Delft University of Technology*, 2007.

[8] J. S. Leendertz and M. H. Kolstrein, "The behaviour of trough stiffener to crossbeam connections in orthotropic steel bridge decks," *Hereon J. Delft Univ. Technol.*, no. 40–3, pp. 217–259, 1995.

[9] R. Wolchuk, "Lessons from Weld Cracks in Orthotropic Decks on Three European Bridges," *J. Struct. Eng.*, vol. 116, no. 1, pp. 75–84, Jan. 1990.

[10] Z. H. Qian and D. Abruzzese, "Fatigue failure of welded connections at orthotropic bridges," *Frat. Ed Integrità Strutt.*, vol. 3, no. 9, pp. 105–112, Jul. 2009.

[11] S. R. Bright and J. W. Smith, "A new design for steel bridge decks using laser fabrication," *Struct. Eng.*, vol. 85, no. 21, pp. 49–57, 2007.

[12] T.-S. Lok and Q.-H. Cheng, "Elastic stiffness properties and behavior of truss-core sandwich panel," *J. Struct. Eng.*, vol. 126, no. 5, pp. 552–559, 2000.

[13] P. Nilsson and M. Al-Emrani, "Industrialized light-weight steel bridge concept using corrugated core steel sandwich plates," *19th IABSE Congr. Stockh.*, 2016.

[14] D. Dackman and W. Ek, "Steel sandwich decks in medium span bridges," *Chalmers University of Technology*, 2015.

[15] D. Ungermann and C. Rüsse, "Zur Dauerhaftigkeit laserstrahlgeschweißter Stahlhohlplatten im Brückenbau," *Stahlbau*, vol. 85, no. 11, pp. 733–739, Nov. 2016.

[16] F. Roland and B. Metschkow, "Laser welded sandwich panels for shipbuilding and structural steel engineering," *Trans. Built Environ.*, vol. 24, pp. 183–194, 1997.

[17] F. Roland and T. Reinert, "Laser welded sandwich panels for the shipbuilding industry," *Lightweight Constr. Dev.*, pp. 24–25, 2000.

[18] F. Roland, T. Reinert, and G. Pethan, "Laser Welding in Shipbuilding – an Overview of the Activities at Meyer Werft," *Proc. IIW Cph.*, 2002.

[19] E. Beneus and I. Koc, "Innovative road bridges with steel sandwich decks," *Chalmers University of Technology*, 2014.

[20] C. Libove and R. Hubka, "Elastic constants for corrugated-core sandwich plates," *NACA TN 2289*, 1951.

[21] K. H. Tan, P. Montauge, and C. Norris, "Steel sandwich panels: finite element, closed solutions and experimental analysis on a 6x2m panel," *Struct. Eng.*, no. 67, pp. 159–189, 1989.

[22] E. M. Knox, M. J. Cowling, and I. E. Winkle, "Adhesively bonded steel corrugated core sandwich construction for marine applications," *Mar. Struct.*, vol. 11, no. 4, pp. 185–204, 1998.

[23] T. S. Lok and Q. H. Cheng, "Elastic Deflection of Thin-Walled Sandwich Panel," *J. Sandw. Struct. Mater.*, vol. 1, no. 4, pp. 279–298, Oct. 1999.

[24] E. W. Reutzel, W. G. Rhoads, and P. A. Blomquist, "LASCORE - The Development of Lightweight Laser Welded Corrugated Panels, Technical Memorandum," *Pa. State Univ.*, 2001.

[25] J. Sikora and A. Dinsenbacher, "SWATH Structure: Navy Research and Development Applications," *Mar. Technol.*, vol. 27, no. 4, pp. 211–220, 1990.

[26] J. Romanoff and P. Kujala, "Formulation for the strength analysis of all steel sandwich panels. Rep. No. M266," *Helsinki University of Technology, Ship Laboratory*, 2002.

[27] J. Romanoff, "Bending response of laser-welded web-core sandwich plates," *Helsinki University of Technology, Ship Laboratory*, Espoo, 2007.

[28] J. Jelovica, "Global buckling response of web-core steel sandwich plates influenced by general corrosion," *Aalto University*, 2014.

[29] D. Frank, "Fatigue strength assessment of laser stake welds in web-core steel sandwich panels," *Aalto University*, 2014.

[30] J. Kozak, "Selected problems on application of steel sandwich panels to marine structures," *Pol. Marit. Res.*, vol. 16, no. 4, Jan. 2009.

[31] SANDCORE, "Best Practice Guide for Sandwich Structures," *Eur. Comm. Contract No FP6-506330*.

[32] SANDWICH, "Advanced composite sandwich steel structures - Public project summary," 2000.

[33] D. Zenkert, "An introducion to sandwich structures," *R. Inst. Technol.*, 1995.

[34] Kenno-tech, [Online]. Available: www.kennotech.fi. [Accessed: 17-feb-2020].

[35] J. Säynäjäkangas and T. Taulavuori, "A review in design and manufacturing of stainless steel sandwich panels," *Stainl. Steel World*, vol. october, 2004.

[36] V. Caccese and S. Yorulmaz, "Laser welded steel sandwich panel bridge deck development: Finite element analysis and stake weld strength tests," *The University of Maine*, 2009.

[37] O. Klostermann, "Zum Tragverhalten von lasergeschweis sten Stahlhohlplatten im Brückenbau," *TU Dortmund*, 2012.

[38] P. Kujala and A. Klanac, "Steel sandwich panels in marine applications," *Brodogradnja*, vol. 56, no. 4, pp. 305–314, 2005.

[39] P. Kujala, S. Ehlers, J. Romanoff, and K. Tabri, "All Steel Sandwich Panels - Design Challenges for Practical Applications on ships." *9th Symposium on Practical Design of Ships and Other Floating Structures*, 2004.

[40] P. Nilsson, M. Al-Emrani, and S. R. Atashipour, "Transverse shear stiffness of corrugated core steel sandwich panels with dual weld lines," *Thin-Walled Struct.*, vol. 117, pp. 98–112, Aug. 2017.

[41] D. Frank, H. Remes, and J. Romanoff, "On the slope of the fatigue resistance curve for laser stake-welded T-joints: ON THE SLOPE OF THE FATIGUE RESISTANCE CURVE," *Fatigue Fract. Eng. Mater. Struct.*, vol. 36, no. 12, pp. 1336–1351, Dec. 2013.

[42] W. Fricke, C. Robert, R. Peters, and A. Sumpf, "Fatigue strength of laser-stake welded T-joints subjected to combined axial and shear loads," *Weld. World*, vol. 60, no. 3, pp. 593–604, May 2016.

[43] J. Kozak, "Strength tests of steel sandwich panel," *Marit. Transp. Exploit. Ocean Coustal Resour.*, 2005.

[44] R. Peters, A. Sumpf, D. Ungermann, C. Rüsse, W. Fricke, and C. Robert, "Laserstrahlgeschweißte T-Stoß-Verbindungen in Stahlhohlplatten: Laserstrahlgeschweißte T-Stoß-Verbindungen in Stahlhohlplatten," *Stahlbau*, vol. 84, no. 9, pp. 643–649, Sep. 2015.

[45] S. P. Abbot, V. Caccese, L. Thompson, P. A. Blomquist, and E. E. Hansen, "Automated laser welded high performance steel sandwich bridge deck development," *TRB Annu. Meet.*, 2008.

[46] A. T. Karttunen, J. N. Reddy, and J. Romanoff, "Two-scale micropolar plate model for web-core sandwich panels," *Int. J. Solids Struct.*, vol. 170, pp. 82–94, Oct. 2019.

[47] A. T. Karttunen, J. N. Reddy, and J. Romanoff, "Micropolar modeling approach for periodic sandwich beams," *Compos. Struct.*, vol. 185, pp. 656–664, Feb. 2018.

[48] G. Socha, K. Koli, and P. Kujala, "Mechanical tests and metallurgical investigation on weld samples," Report AWCS-Project No. BE 96-3932-Task A4, 1998.

[49] CEN, "Eurocode 3: Design of steel structures - Part 1-9: Fatigue," Brussels: *European Committee for Standardization* (CEN), 2005.

[50] A. F. Hobbacher, "Recommendations for Fatigue Design of Welded Joints and Components (IIW document IIW-2259-15)," 2nd ed. Switzerland: Springer International Publishing, 2016.

[51] D. Radaj, C. M. Sonsino, and W. Fricke, "Fatigue assessment of welded joints by local approaches," Cambridge, England: Woodhead, 2006.

[52] M. Al-Emrani and M. Aygül, "Fatigue design of steel and composite bridges," *Chalmers Univ. Technol. Dep. Civ. Environ. Eng. Göteb.*, 2014.

[53] D. Frank, H. Remes, and J. Romanoff, "Fatigue assessment of laser stake-welded T-joints," *Int. J. Fatigue*, vol. 33, no. 2, pp. 102–114, Feb. 2011.

[54] P. Lazzarin and P. Livieri, "Notch stress intensity factors and fatigue strength of aluminium and steel welded joints," *Int. J. Fatigue*, vol. 23, no. 3, pp. 225–232, Mar. 2001.

[55] D. Frank, P. Dissel, H. Remes, J. Romanoff, and O. Klostermann, "Fatigue strength assessment of laser stake-welded T-joints subjected to reversed bending: Laser Stake-Welded T-Joints Under Reversed Bending," *Fatigue Fract. Eng. Mater. Struct.*, vol. 39, no. 10, pp. 1272–1280, Oct. 2016.

[56] D. Frank, J. Romanoff, and H. Remes, "Fatigue strength assessment of laser stake-welded web-core steel sandwich panels," *Fatigue Fract. Eng. Mater. Struct.*, vol. 36, no. 8, pp. 724–737, Aug. 2013.

[57] D. Frank, H. Remes, and J. Romanoff, "J-integral-based approach to fatigue assessment of laser stake-welded T-joints," *Int. J. Fatigue*, vol. 47, pp. 340–350, Feb. 2013.

[58] S. R. Bright and J. W. Smith, "Fatigue performance of laser-welded steel bridge decks," *Struct. Eng.*, vol. 2004, pp. 31–38, 2004.

[59] J. Kozak, "Fatigue life of steel laser-welded panels," *Pol. Marit. Res.*, pp. 13–16, 2006.

[60] S. Gunecha, "Corrugated core sandwich steel panel - Quantifying performance improvment between empty and filled sandwich panels using J-integral based local approach," *Delft University of Technology*, 2019.

[61] R. Frank, J. Romanoff, and R. Heikki, "Fatigue life improvement of laser-welded web-core steel sandwich panels using polymer-based filling material," *IIW Doc. XIII-2598-15*, vol. 2015.

[62] J. Romanoff and P. Varsta, "Bending response of web-core sandwich beams," *Compos. Struct.*, vol. 73, no. 4, pp. 478–487, Jun. 2006.

[63] J. Romanoff, P. Varsta, and A. Klanac, "Stress analysis of homogenized web-core sandwich beams," *Compos. Struct.*, vol. 79, no. 3, pp. 411–422, Jul. 2007.

[64] J. Romanoff, H. Remes, G. Socha, M. Jutila, and P. Varsta, "The stiffness of laser stake welded T-joints in web-core sandwich structures," *Thin-Walled Struct.*, vol. 45, no. 4, pp. 453–462, Apr. 2007.

[65] J. Romanoff and P. Varsta, "Bending response of web-core sandwich plates," *Compos. Struct.*, vol. 81, no. 2, pp. 292–302, Nov. 2007.

[66] J. Romanoff, P. Varsta, and H. Remes, "Laser-welded web-core sandwich plates under patch loading," *Mar. Struct.*, vol. 20, no. 1–2, pp. 25–48, Jan. 2007.

[67] N. Buannic, P. Cartraud, and T. Quesnel, "Homogenization of corrugated core sandwich panels," *Compos. Struct.*, vol. 59, no. 3, pp. 299–312, 2003.

[68] L. He, Y.-S. Cheng, and J. Liu, "Precise bending stress analysis of corrugated-core, honeycomb-core and X-core sandwich panels," *Compos. Struct.*, vol. 94, no. 5, pp. 1656–1668, Apr. 2012.

[69] B. Reinaldo Goncalves and J. Romanoff, "Size-dependent modelling of elastic sandwich beams with prismatic cores," *Int. J. Solids Struct.*, Dec. 2017.

[70] A. T. Karttunen, J. N. Reddy, and J. Romanoff, "Two-scale constitutive modeling of a lattice core sandwich beam," *Compos. Part B Eng.*, vol. 160, pp. 66–75, Mar. 2019.

[71] M. Minnicino and D. Hopkins, "Overview of Reduction Methods and Their Implementation Into Finite-Element Local-to-Global Techniques:," Defense Technical Information Center, Fort Belvoir, VA, Sep. 2004.

[72] H. G. Allen, "Analysis and design of structural sandwich panels." Pergamon Oxford, 1969.

[73] F. J. Plantema, "Sandwich construction," New York: John Wiley & Sons, 1966.

[74] J. R. Vinson, "The behavior of sandwich structures of isotropic and composite materials," Lancaster: Technomic, cop. 1999, 1999.

[75] J. N. Reddy, "Mechanics of laminated composite plates and shells – Theory and analysis," 2nd ed. Boca Raton: CRC Press, 2004.

[76] A. K. Noor, W. S. Burton, and C. W. Bert, "Computational models for sandwich panels and shells," *Appl. Mech. Rev.*, vol. 49, no. 3, pp. 155–199, 1996.

[77] J. R. Vinson, "Sandwich structures," *Appl. Mech. Rev.*, vol. 54, no. 3, pp. 201–214, 2001.

[78] C. Libove and S. B. Batdorf, "A general small-deflection theory for flat sandwich plates," *NACA Rep. No 899*, 1948.

[79] E. Reissner, "The effect of transverse shear deformation on the bending of elastic plates," *J. Appl. Mech.*, no. 12, pp. 69–77, 1945.

[80] R. D. Mindlin, "The influence of Rotary Inertia and Shear on Flexural Motions of Isotropic, Elastic plates," *J. Appl. Mech.*, vol. 18, pp. 31–38, 1951.

[81] M. Stein and J. Mayers, "A small-deflection theory for curved sandwich plates," NACA vol. 1008, 1951.

[82] W.-S. Chang, E. Ventsel, T. Krauthammer, and J. John, "Bending behavior of corrugated-core sandwich plates," *Compos. Struct.*, vol. 70, no. 1, pp. 81–89, Aug. 2005.

[83] D. J. O'Connor, "Point concentrations in thick-faced sandwich beams," *J. Eng. Mech.*, vol. 114, no. 5, pp. 733–752, 1988.

[84] Å. Holmberg, "Shear-weak beams on elastic foundation," *IABSE Publ.*, vol. 10, 1950.

[85] T.-S. Lok, Q. Cheng, and L. Heng, "Equivalent Stiffness Parameters of Truss-Core Sandwich Panel," *Proc. Ninth 1999 Int. Offshore Polar Eng. Conf.*, pp. 292–298, 1999.

[86] P. Kujala, A. Klanac, and others, "Analytical and numerical analysis of non-symmetrical all steel sandwich panels under uniform pressure load," in *DS 30: Proceedings of DESIGN 2002, the 7th International Design Conference, Dubrovnik*, 2002.

[87] T. Nordstrand, L. A. Carlsson, and H. G. Allen, "Transverse shear stiffness of structural core sandwich," *Compos. Struct.*, vol. 27, no. 3, pp. 317–329, 1994.

[88] S. P. Timošenko and S. Woinowsky-Krieger, "Theory of plates and shells," 2. ed., Internat. ed. Auckland: McGraw-Hill, 1976.

[89] S. R. Atashipour and M. Al-Emrani, "A realistic model for transverse shear stiffness prediction of composite corrugated-core sandwich elements," *Int. J. Solids Struct.*, vol. 129, pp. 1–17, Dec. 2017.

[90] L. Sandberg and A. Palmkvist, "Fatigue Analysis of Hybrid Laser Welds in Steel Sandwich Bridge Decks," *Chalmers University of Technology*, Göteborg, 2015.

[91] L. Persson, "A parametric study of shear-induced fatigue in corrugated steel sandwich elements," *Chalmers University of Technology*, Göteborg, Sweden, 2016.

[92] A. W. M. Kok and J. Blaauwendraad, "Shape-orthotropic stressing–bending plate model," *Eng. Struct.*, vol. 30, no. 10, pp. 2884–2892, Oct. 2008.

[93] CEN, "EN 1990/A1: Eurocode - Basis of structural design,". Bruselles, Belgium: European Committee for Standardization CEN, 2005.

[94] CEN, "Eurocode 3: Design of steel structures - Part1-5: Plated structural elements," European Committee for Standardization CEN, 2009.

[95] A. Zizza, "Buckling behaviour of unstiffened and stiffened steel plates under multiaxial stress state," *University of Stuttgart*, 2016.

[96] D. N. Veritas, "Buckling strength of plated structures," *Recomm. Pract. DNV-RPC201 Høvik Nor.*, 2002.

APPENDED PAPERS